A LASER BASED, NON-INVASIVE MEASUREMENT OF BLOOD PERFUSION

by

Gregory T. Martin

Bachelor of Science, Massachusetts Institute of Technology
1988

SUBMITTED TO THE DEPARTMENT OF
MECHANICAL ENGINEERING IN PARTIAL
FULFILLMENT OF THE REQUIREMENTS FOR THE
DEGREE OF

MASTER OF SCIENCE

at the

MASSACHUSETTS INSTITUTE OF TECHNOLOGY

June 1991

Signature Redacted

Signature of Author

Department of Mechanical Engineering
June 3, 1991

Signature Redacted

Certified by

H. Frederick Bowman
Thesis Supervisor

Signature Redacted

Accepted by

Professor Anin Sonin
Chairman, Graduate Thesis Committee

A LASER BASED, NON-INVASIVE MEASUREMENT OF BLOOD PERFUSION

by

Gregory T. Martin

Submitted to the Department of Mechanical Engineering on June 3, 1991 in partial fulfillment of the requirements for the degree of Master of Science.

Abstract

A method for the quantification of tissue perfusion is presented and evaluated. Perfusion, which is the volumetric flow of blood through the tissue per unit of tissue volume, is a carrier of heat and mass (nutrients) in the chain of tissue transport. Knowledge of the tissue perfusion is important to all clinical procedures which depend on heat and mass transport. This perfusion measurement method is a thermal diffusion technique in which a small quantity of heat is introduced into the tissue by laser irradiation of the tissue surface. The surface temperature is then monitored either via a non-contact mode with an infrared detector or via a non-invasive contact mode with a surface thermistor. A model of the tissue thermal interactions allows for the quantification of perfusion.

The model is developed for two different cases of laser-tissue interaction. The first case is where all the laser energy is absorbed at the tissue surface. The second case is where the laser energy is attenuated within the tissue according to the Kubelka-Munk theory. An exact analytical solution of the model for transient and steady state is given. The solutions are arrived at by a Hankel integral transform of the governing equations. The solutions are used to determine the parameters which maximize the sensativity of the tissue surface temperature to perfusion. It is found that the sensativity of temperature to perfusion is maximized by using a laser wavelength which penetrates deep into the tissue.

To test the validity of the perfusion measurement method, an experimental protocol is inplemented. The protocol uses an albino rat liver, fixed in an ethyl alcohol solution and perfused with distilled water to model the tissue. A dye laser operating at at 647 nm is used to slightly heat the liver surface. The temperature is recorded with a thermistor mounted on the tissue surface. In agreement with the model, it was found that for volumetric laser heating of the tissue, surface temperature has a strong dependence on perfusion. This dependence of surface temperature on perfusion can be exploited in the development of this measurement technique.

Thesis Supervisor: H. Frederick Bowman
Title: Lecturer of Mechanical Engineering

Table of Contents

List of Figures

List of Tables

Acknowledgement

In the undertaking of this work, I have depended on a number of people and institutions. Here I will attempt to recognize their support for this project

Chapter 1

Introduction and Preliminary Remarks

The living organism is part of the physical world;
it is made up of systems of atoms moved by attractive
and repulsive forces, following the principles of
conservation of energy.
     -Helmholtz

The topic of this thesis is the use of engineering principles applied to the human body to obtain diagnostic information about the state of the body. In this introductory chapter, first the basis of engineering in medicine is discussed with a concentration on heat and mass transfer analysis. Second, the role of blood perfusion in physiology is presented along with the motivation for the quantification of perfusion. Third, various methods of perfusion measurement are described, including the laser based, non-invasive measurement.

1.1 The Human Body as a System

Western medicine views the human body as inherently a chemical system. The chemical basis of the body derives from the building block of physiologic tissue; the eukaryotic cell. Sustaining the cell requires the chemical environment of the cell be suitable. The maintenance of the chemical environment is of primary importance for all cells, tissues and physiological processes. A favorable chemical environment is one which supplies nutrients, disposes of waste, and maintains an optimum temperature.

Within the realm of human physiology, one can define and analyze a number of systems. Never are these systems capable of being clearly defined and analyzed with exactitude because many interactions occur among systems. However, some commonly defined macroscopic systems are cardiovascular, respiratory, nervous, gastro-intestinal, renal, skeletal, etc. One can apply various analysis tools to each of these systems or

domains in order to gain an insight into the system performance. Examples of such tools are solid mechanics, fluid mechanics, system dynamics, control theory and heat and mass transfer. In this thesis the principles of heat and mass transfer are applied to the cardiovascular system.

1.2 Bioheat and Mass Transfer

Bioheat and mass transfer comprehends a set of analysis tools which can be applied throughout the body. These analysis tool can be quite powerful due to the thermodynamic and chemical basis of the body and the dependence of the body on heat and mass transport. The principles of transport phenomenon are manifest at all levels of physiologic processes: from the intercellular to the inter-organal; from the transport of macromolecules across the cell membrane to the flow of blood in the aorta.

As pragmatists, we are interested in using the principles of heat and mass transfer to obtain diagnostic information about the body as well as to treat some diseased condition. For diagnosis, the current state of the physiologic system is compared with a known healthy reference state. Deviations from the reference state are recognized as a diseased state and can then be subject to beneficial interventions (treatment). For treatment, heat or mass is interjected into or removed from the system to elicit a healthy physiologic response. The pragmatic, or engineering approach, is in contrast to the purely scientific approach where information is gathered simply as an end in itself.

In this thesis, a method of measuring blood perfusion is presented and evaluated. The measurement method employs the principles of heat and mass transfer applied to tissue. The goal of perfusion measurement is to provide diagnostic information to determine the state of the tissue.

1.3 Perfusion

In physiologic tissue, blood is carried by the arteries and arterioles to the capillary beds. The small dimensions of the capillaries in the tissue allow for mass transport by diffusion and osmosis within a time scale which is biologically feasible. The capillaries then empty into the venules and on into the veins. This flow of blood through the capillary beds is called perfusion. Perfusion can be quantified as a volume flow of blood per unit volume of tissue which surrounds the capillary bed. Often perfusion is given units of *ml of blood per min per 100 ml of tissue*. In this form, the perfusion is a percentage of tissue volume which flows through the tissue volume each minute.

1.4 Motivation

1.4.1 Assessment of Organ Transplant Success

One of the crowning achievements of medicine over the past twenty years has been to make major organ transplantation a commonplace event. Given that there exists a compatible donor, such organs as the kidney, liver, heart or lung, can be transplanted to a needy recipient. The transplant of skin for a skin graft is common and has been done for the past eighty years. Following the transplant of tissue (6 to 12 hours) the clinician must determine if there are vascular complications in the transplanted tissue. Typically, post-operative monitoring focuses on the large vessel blood flow of the transplanted tissue. However, focusing on the large vessel flow will not recognize reduced flow in the pre-capillary arterioles or the post-capillary venules. Only the quantification of the transplanted tissue perfusion provides an accurate, objective and atraumatic assessment of the transplantation [43].

1.4.2 Hyperthermia Treatment

It has been found that some neoplastic cells are more susceptible to heat damage than normal cells. Thus an entire genre of tumor treatment has been developed around the elevation of tissue temperature to within a therapeutic window. Once tissue is uniformly sustained at this therapeutic temperature for some treatment time, tumor cells are selectively killed while the healthy tissue cells are spared. The actual value of the temperature increase has been the subject of some debate but the elevated temperature is around 43° C. Usually the tissue heating is achieved by irradiating the tissue with microwaves, radiowaves, ultrasound, or laser light [49].

In response to tissue heating, blood flow is the primary mechanism for thermal regulation. Perfusion provides an important component for this regulation [4, 46]. Any hyperthermia heating mechanism must be able to supply sufficient energy to compensate for the heat carried away by blood flow. Also the heating mechanism must differentially deposit energy in response to changes in tissue perfusion over time and space. Thus during any hyperthermia treatment, constant monitoring of the perfusion is required to achieve the desired therapeutic temperature elevation in the tumor.

1.5 Methods of Perfusion Measurement

1.5.1 Laser-Doppler

The laser-Doppler technique can be used to measure velocity of a moving particle. The velocity of a particle is determined by shining a beam of light on the particle and measuring the Doppler shift of the backscattered light. With regard to the measurement of perfusion, the Doppler shift is produced by the interaction of the laser light with the moving erythrocytes in the tissue. The laser-Doppler signal is thus proportional to the product of the number of moving erythrocytes and the average cell velocity [45, 9]. Knowledge of the

blood hematocrit and the laser-Doppler signal gives the average erythrocyte velocity which is then used as a gauge of the blood perfusion.

1.5.2 Indicator Dilution

The indicator dilution techniques for measuring perfusion usually introduce a known quantity of a substance into the tissue (such as dyes, radioactive indicators or heat) and measure the concentration of the substance in the tissue as a function of space and/or time. The substance concentration is related to perfusion through the principle of mass (or energy) conservation.

1.5.2.1 Radioactive Indicator

A common method of indicator dilution measurement of perfusion utilizes radioactive microspheres. These microspheres, usually with a diameter of 5-100 μm and made out of albumin labeled with iodine^{131} or technitium^{99m}, are injected into the vascular system and become trapped in the capillary beds. A radioactive image can then be recorded on radiographic film, photographic film or videotape. The radioactive image gives relative information about the flow patterns and distribution of blood in the tissue [31].

1.5.2.2 Thermal Indicator

The thermal indicator (diffusion) methods to measure perfusion involve introducing a known quantity of heat into the tissue and then measuring the change in tissue temperature. A common thermal diffusion method uses an electrical resistive thermistor fastened to a probe which is inserted into the tissue. A known quantity of electrical energy is used to heat the thermistor to a measured and constant temperature slightly above the initial thermal equilibrium temperature of the tissue and the thermistor. A heat transfer model of the thermistor and tissue then allows for the solution of the effective thermal conductivity of the tissue and the blood perfusion [3, 54]. The thermal diffusion technique gives an absolute and accurate measure of the perfusion and is thus superior to the laser-Doppler and the radioactive microsphere methods which only provide relative information.

1.6 The Laser Based, Non-Invasive Measurement of Perfusion

The non-invasive measurement of perfusion is a thermally based method. A known quantity of heat is introduced into the tissue by a laser and the subsequent rise in tissue temperature is recorded. A heat transfer model of the tissue thermal interactions is used to determine the blood perfusion. The temperature rise of the tissue is small enough (about 5 C) such that there is no phase change, chemical breakdown, pressure waves, nor plasma formation in the tissue. Also it is assumed that there is no physiologic response to the localized heating in the form of increased blood perfusion.

It is always desirable to make measurements non-invasively, in order to minimize the perturbation of the measured system. In biomedical engineering, non-invasive measurements are particularly important to minimize the patient trauma and to reduce the risk of infection. The non-invasive perfusion measurement is actually thermally invasive while being mechanically non-invasive.

1.6.1 Previous Investigations

There has been sporadic investigation on using material thermal response to laser irradiation as measurement of thermal properties. Hansen, Greenwald and Bowman [16] used a CO_2 laser to heat an agar gel. The temperature rise was monitored with a thermocouple inserted into the medium. A heat transfer model of the laser heating was used to determine the thermal conductivity They reported good agreement between measured and actual thermal conductivity (8%).

Kamada et al [19] used an argon ion laser to heat, in-vivo, a rat liver. The temperature rise was monitored with a infrared camera. No attempt was made to quantify the tissue thermal properties or blood perfusion, though the thermal response of the tissue as a function of perfusion was qualitatively discussed.

Leung and Tam [24, 25] used a pulsed N_2 laser to heat thin samples of material. The thermal response was monitored with a single element infrared detector. They present a detailed analytical model of the material thermal response with the aim of quantifying the material thickness and thermal diffusivity.

Long, Nishioka and Deutsch [26] applied the technique of pulsed photothermal radiometry of Leung and Tam to the measurement of the optical and thermal properties of biliary calculi. They reported good agreement for the thermal diffusivity and optical absorption (15%) with reference material samples.

NASA [34] has developed a laser anemometer device for the measurement of the fluid boundary layer around a wind tunnel specimen. The device uses a laser to heat up the specimen and an infrared imager to measure the thermal response. They present a heat transfer model from which the boundary layer thickness can be determined. The authors suggest that this system can also be used to measure the thermal properties of materials.

Though an extensive literature search was conducted, little work has been found on the thermal modeling of blood perfused, laser irradiated tissue. Such a model would serve as a basis for the quantification of perfusion from the thermal response of laser heated tissue. Welch, Wissler and Priebe [58] used a convolution integral solution of the bioheat equation to demonstrate the significance of perfusion in the thermal response of laser irradiated tissue. They show that for laser exposure times less than 8 seconds at medium levels of perfusion, the thermal response of tissue is not significantly affected by perfusion. Martin and Bowman [28, 29] used an integral transform solution of the bioheat equation to give a complete description of the thermal response of blood perfused tissue. They show that the thermal response of tissue is made more sensitive to perfusion by heating with a laser which penetrates into the tissue.

The aim of this thesis is to develop a methodology for the quantification of perfusion using a laser as a non-contact heat source. This aim is similar to Kamada et al, however,

this thesis stresses the thermal modeling as well as the experimental protocol for perfusion measurement. The thermal modeling is taken from Martin and Bowman and reproduced in Chapter 2.

1.6.2 Overall Description

Figure 1-1 shows diagrammatically the measurement system. The laser provides a controllable and quantifiable heat source which can be directed down slender optical fibers into intercavernous ducts. The surface temperature measurement can be made with a thermistor mounted on the tissue surface. If a non-contact temperature measurement is required, an infrared detector can be used at the expense of temperature resolution. The recent advances in infrared optical fibers make remote infrared sensing possible [60, 20, 50].

In order to determine the perfusion from the experiment in Figure 1-1, the laser-tissue interaction and the heat transfer mechanisms in the tissue must be modeled. From the model and the experimental parameters, the perfusion can be determined.

In the next chapter the heat transfer model for the laser heating of blood perfused tissue is presented. In Chapter 3, the model is evaluated to determine the optimal parameters for the non-invasive measurement. In Chapter 4, the experimental protocol is presented along with the results and discussion. The thesis concludes with Chapter 5, which contains a summary of the work and a discussion on the future of the non-invasive measurement.
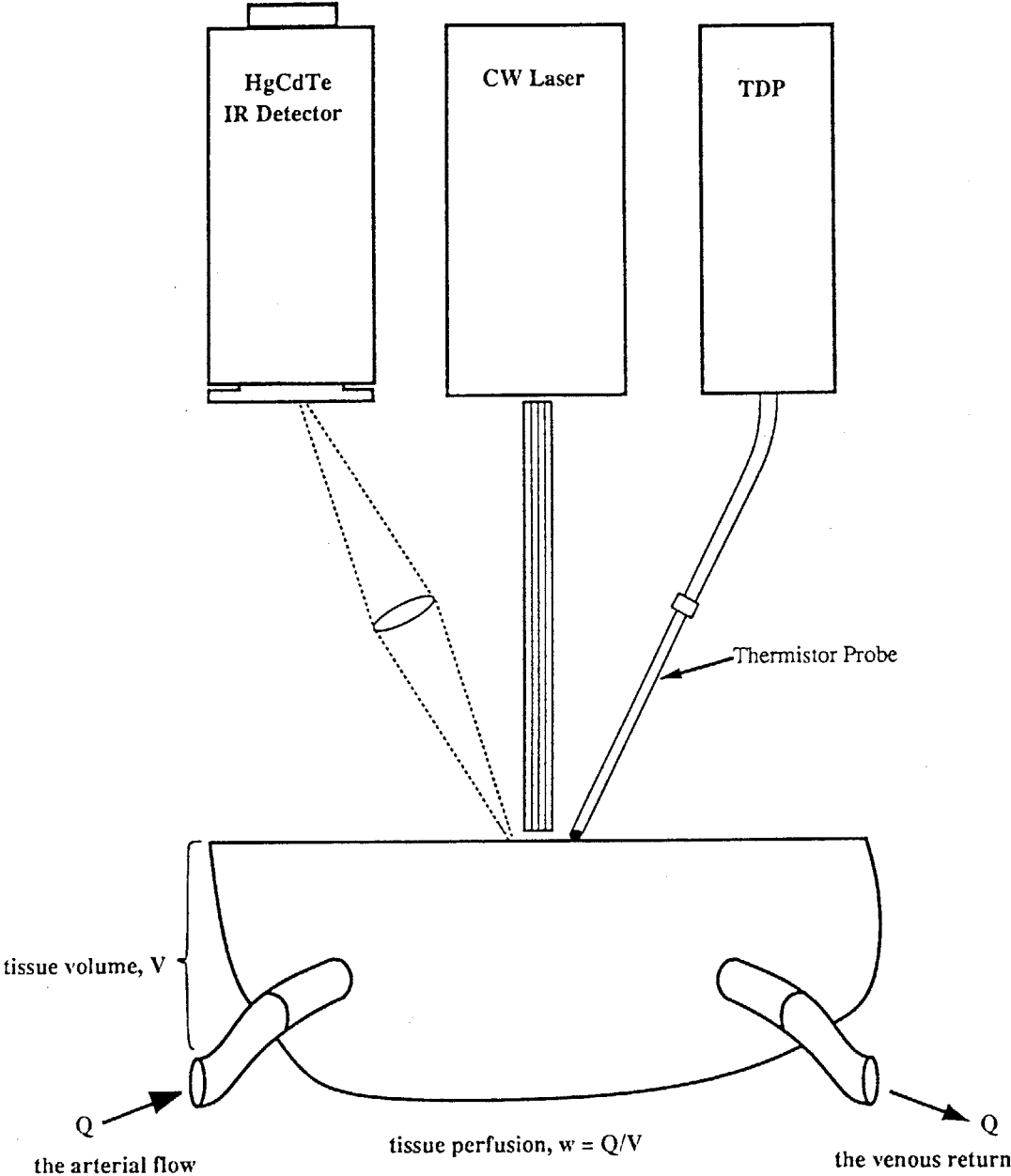
Figure 1-1: Schematic diagram of the non-invasive perfusion measurement system.

Chapter 2

Model and Solution for the Thermal Response of Tissue

In this chapter, the thermal response of perfused tissue during continuous wave laser heating is modeled. The distribution of laser energy in the beam is assumed to be Gaussian. Two separate models of the laser-tissue interaction are developed; one for the case where all the laser energy is converted to thermal energy at the surface of the tissue and the second for the case where the laser energy penetrates into the tissue where thermal dissipation takes place (volumetric absorption). In both cases the tissue is modeled as a semi-infinite body which is homogeneously perfused by blood.

The present solution is arrived at by the methods of separation of variables and the Hankel integral transform. This approach reveals a solution form which need only be integrated over the eigenvalues as opposed to a Green's function solution which must be integrated over space and time. Further, the present solution is exact and requires far less computation time then the approximate finite element and finite difference solutions.

2.1 Surface Absorption of Laser Energy

2.1.1 Laser-Tissue Interaction

The distribution of power density within the laser beam is the well known Gaussian distribution for a laser operating in the lowest order mode [42]:

$$I(r) = I_o e^{-2r^2/\sigma^2} \tag{2.1}$$

where I_o is the power density at $r=0$ and σ is the $1/e^2$ radius of the beam.

The attenuation of radiation in a medium results from a conversion of the radiant energy into thermal energy. If the absorption of the laser energy is sufficiently high, it can

be assumed that all of the laser energy is absorbed at the surface. This assumption is particularly valid for the case of a CO_2 laser incident upon tissue with a high water content or an ultra violet (UV) laser incident on tissue with a high protein content. Equation (2.1) will therefore describe the heat flux at the surface of the tissue in the case where all laser energy is absorbed at the surface.

2.1.2 Bioheat Transfer

The tissue is modeled as a homogeneous semi-infinite body. It is assumed that the capillaries are oriented in a random fashion and the arterioles and venules do not contribute to the local heat transfer, thus the convective heat transfer due to perfusion is non-directional. Further, it is assumed that the baseline temperature of the tissue is in equilibrium with the incoming arterial blood. The effect of perfusion on the local tissue heat transfer is modeled as a linear temperature dependent heat sink [41].

The effect of perfusion on the local tissue heat transfer is a well discussed issue. Of course, an ideal model would be valid over all space, all time and all values of perfusion. The reality is that the present formulation of the bioheat transfer equation is valid for small volumes of heated tissue (with a characteristic length between 0.1 cm and 1 cm) and at low rates of perfusion (below 100 ml/100 ml of tissue-min).

At the surface, it is assumed that natural convection and radiant heat transfer from the tissue are negligible compared to the incident laser power. Also, there is no forced convection at the surface and the thermal conductivity of the tissue is much greater than the thermal conductivity of air. The temperature rise in the tissue is assumed to be small enough such that there are no phase changes, chemical reactions, mass transport, or mechanical effects.

2.1.3 Formulation of Governing Equations

The governing equations are formulated in cylindrical coordinates with the origin at the point in the surface of the tissue where the laser beam intensity is greatest. The laser beam intensity is symmetric about the z axis and the tissue properties and the perfusion are homogeneous, thus the temperature does not change as a function of θ. The bioheat transfer equation takes the form:

$$\frac{\partial^2 T}{\partial r^2} + \frac{1}{r}\frac{\partial T}{\partial r} + \frac{\partial^2 T}{\partial z^2} - \frac{\omega \rho_b c_b}{k_m} T = \frac{1}{\alpha}\frac{\partial T}{\partial t} \qquad (2.2)$$

where T is the temperature rise, ρ_b is the density of blood, c_b is the specific heat of blood, ω is the blood perfusion rate, k_m is the tissue intrinsic thermal conductivity and α is the intrinsic tissue thermal diffusivity.

The boundary conditions are (1) at the body surface the heat source is given by equation (2.1), (2) as the spatial dimensions approach infinity the temperature rise approaches zero, (3) the temperature field is symmetric about the z axis, and (4) at t equal to zero the temperature rise everywhere is zero. The equivalent mathematical statements of the boundary conditions are as follows.

$$-k_m \frac{\partial T}{\partial z}_{z=0} = I_o e^{-2r^2/\sigma^2} \qquad (2.3)$$

$$T(r=\infty, z, t) = 0 \qquad (2.4)$$

$$T(r, z=\infty, t) = 0 \qquad (2.5)$$

$$\frac{\partial T}{\partial r}_{r=0} = 0 \qquad (2.6)$$

$$T(r, z, t=0) = 0 \qquad (2.7)$$

2.1.4 Solution procedure for the steady state temperature

Since the boundary conditions are homogeneous, the temperature can be expressed as the product of a function of r, a function of z and a constant function. The product is substituted into equation (2.2) to obtain two independent ordinary differential equations.

$$T(r,z) = g(r) \, h(z) \, f(\lambda) \tag{2.8}$$

$$g''(r) + \frac{1}{r} g'(r) - g(r) \beta^2 = 0 \tag{2.9}$$

$$h''(z) - \lambda^2 h(z) = 0 \tag{2.10}$$

$$\beta = \sqrt{\lambda^2 + \frac{\omega \rho_b c_b}{k_m}}$$

where λ is the eigenvalue. The equations (2.9) and (2.10) can be solved with the boundary conditions of equations (2.4), (2.5), and (2.6) to reveal the functions $g(r)$ and $h(z)$. The steady state temperature distribution is arrived at by integrating the g(r), h(z) and f(λ) functions over permissible eigenvalues.

$$T(r,z) = g(r) \, h(z) \, f(\lambda) = \int_0^\infty J_o(\lambda r) \, e^{-\beta z} f(\lambda) \, d\lambda \tag{2.11}$$

where J_0 is the zero order Bessel function.

The function f(λ) can be found if it is recognized that the boundary condition of equation (2.3) is equivalent to the Weber integral of the first kind [55, 36] which gives f(λ). The complete solution for the steady state temperature distribution is:

$$T(r,z) = \frac{I_o \sigma^2}{4 k_m} \int_0^\infty \lambda J_o(\lambda r) \, e^{-z\beta} \, e^{-\sigma^2 \lambda^2 / 8} \frac{d\lambda}{\beta} \tag{2.12}$$

In most cases, equation (2.12) must be evaluated numerically. It should be noted that as the perfusion goes to zero, the solution for temperature distribution becomes the solution of [30].

Oftentimes it is convenient to represent the solution for temperature in dimensionless form. Such a representation is:

$$\theta = \frac{1}{4} \int_0^\infty \lambda J_o(\lambda r_x) \, e^{-z_x v} \, e^{-\lambda^2/8} \frac{d\lambda}{v} \tag{2.13}$$

where

$$\theta = \frac{T k_m}{\sigma I_o}$$

$$r_x = r/\sigma$$

$$z_x = z/\sigma$$

$$v = \sqrt{\lambda^2 + Pe}$$

$$Pe = \frac{\omega \rho_b c_b \sigma^2}{k_m}$$

The quantity Pe much like the Peclet number which characterizes the ratio of convected heat in a fluid to conducted heat.

If it is assumed that there is heat convection at the tissue surface where the cooling fluid temperature is equal to the baseline tissue temperature, then the boundary condition of equation (2.3) becomes:

$$-k_m \frac{\partial T}{\partial z_{z=0}} = I_o e^{-2r^2/\sigma^2} - h \, T(r, z = 0) \tag{2.14}$$

where h is the average heat transfer coefficient at the tissue surface. Equation (2.11) can be resolved with the heat convection boundary condition of equation (2.14). The resulting temperature distribution is:

$$T(r,z) = \frac{I_o \sigma^2}{4 k_m} \int_0^\infty \lambda J_o(\lambda r) \, e^{-z\beta} \, e^{-\sigma^2 \lambda^2/8} \frac{d\lambda}{\beta + h/k_m} \tag{2.15}$$

And the temperature distribution with surface convection can also be put in dimensionless form.

$$\theta = \frac{1}{4} \int_0^\infty \lambda J_o(\lambda r_x) \, e^{-z_x v} \, e^{-\lambda^2/8} \, \frac{d\lambda}{v + Bi}$$ (2.16)

$$Bi = \frac{h\sigma}{k_m}$$

The quantity Bi is the Biot number for the tissue which characterizes the ratio of surface convection to conduction heat transfer.

2.1.5 Solution procedure for the transient temperature

The solution procedure for transient temperature begins with a separation of temperature into a function of r, a function of z and t, and a constant function.

$$T(r,z,t) = g(r)h(z,t)f(\lambda) = \int_0^\infty J_o(\lambda r) e^{-\beta z} \, erfc[\frac{z}{2\sqrt{\alpha t}} - \beta\sqrt{\alpha t}]$$
$$- e^{\beta z} \, erfc[\frac{z}{2\sqrt{\alpha t}} + \beta\sqrt{\alpha t}]f(\lambda) \, d\lambda$$ (2.17)

where *erfc* is the error function compliment. The $h(z,t)$ function is taken from [6], who present a solution for the transient temperature distribution in a semi-infinite body with a disk heat source at the surface. The function $h(z,t)$ is also valid in the case of transient temperature distribution for a Gaussian heat source with blood perfusion, because $h(z,t)$ satisfies equation (2.2) and it will be shown later that the functional form of $h(z,t)$ also satisfies the boundary conditions (equations (2.3), (2.4), (2.5), (2.6) and (2.7)).

The transient temperature is thus given as:

$$T(r,z,t) = \int_0^\infty J_o(\lambda r)f(\lambda) \, \{e^{-\beta z} \, erfc[\frac{z}{2\sqrt{\alpha t}} - \beta\sqrt{\alpha t}]$$
$$- e^{\beta z} \, erfc[\frac{z}{2\sqrt{\alpha t}} + \beta\sqrt{\alpha t}]\} \, d\lambda$$ (2.18)

The function $f(\lambda)$ can be found from the boundary condition of equation (2.4) which is also equivalent to the Weber integral of the first kind [55, 36]. Thus the solution for the transient temperature distribution is:

$$T(r, z, t) = \frac{I_o \sigma^2}{8k_m} \int_0^\infty J_o(\lambda r) e^{-\sigma^2 \lambda^2/8} \{ e^{-\beta z} erfc[\frac{z}{2\sqrt{\alpha t}} - \beta \sqrt{\alpha t}]$$
$$- e^{\beta z} erfc[\frac{z}{2\sqrt{\alpha t}} + \beta \sqrt{\alpha t}] \} \frac{\lambda \, d\lambda}{\beta}$$

(2.19)

As with the steady state solution, in most cases the transient solution must be evaluated numerically. The dimensionless form of equation (2.19) is:

$$\theta = \frac{1}{8} \int_0^\infty J_o(\lambda r_x) e^{-\lambda^2/8} \{ e^{-vz} erfc[\frac{z_x}{2\sqrt{Fo}} - v\sqrt{Fo}]$$

(2.20)

$$- e^{vz_x} erfc[\frac{z_x}{2\sqrt{Fo}} + v\sqrt{Fo}] \} \frac{\lambda \, d\lambda}{v}$$

$$Fo = \frac{\alpha t}{\sigma^2}$$

where Fo is the Fourier number.

It should be noted that as t goes to infinity, equation (2.19) reduces to the steady state solution of equation (2.12). Also, when perfusion goes to zero, equation (2.19) becomes the solution of [30].

2.2 Volumetric Absorption of Laser Energy

2.2.1 Laser-Tissue Interaction

The distribution of laser intensity within the beam is again assumed to be Gaussian (equation (2.1)). A mathematical model which describes the absorption of laser energy within the tissue is used to determine the spatial distribution of the heat deposition. The laser intensity within the tissue is assumed to be given by the Kubelka-Munk theory as applied to laser-tissue interaction in an optically semi-infinite body [56]:

$$I(r,z) = I_o e^{-2r^2/\sigma^2} e^{-z(A(A+2S))^{1/2}}$$

(2.21)

where A is the absorption coefficient and S is the scattering coefficient. For simplicity in notation, the parameter B is defined.

$$B = A(A+2S))^{1/2}$$

Since energy is conserved, the volumetric heat generation within the tissue is equal to the change in laser intensity as a function of z.

$$q(r,z) = -\frac{\partial I(r,z)}{\partial z} = B I_o e^{-2r^2/\sigma^2} e^{-zB} \tag{2.22}$$

2.2.2 Bioheat Transfer

With regard to the heat transfer mechanisms in the tissue, the same assumptions are made here as in the case of surface absorption in Section 2.1.2.

2.2.3 Formulation of Governing Equations

As with the case of surface absorption of laser energy, the governing equations are formulated in cylindrical coordinates with the origin at the point on the tissue surface where the laser intensity is greatest. The governing equations are symmetric about the z axis and thus independent of the θ coordinate. The bio-heat transfer equation is:

$$\frac{\partial^2 T}{\partial r^2} + \frac{1}{r}\frac{\partial T}{\partial r} + \frac{\partial^2 T}{\partial z^2} - \frac{\omega \rho_b c_b}{k_m}T + \frac{B I_o}{k_m} e^{-2r^2/\sigma^2} e^{-zB} = \frac{1}{\alpha}\frac{\partial T}{\partial t} \tag{2.23}$$

The boundary conditions are (1) there is no heat flow out the tissue surface, (2) the temperature field is symmetric about the z axis, (3) as the spatial dimensions approach infinity the temperature rise approaches zero, and (4) at t equal to zero the temperature rise everywhere in space is zero. The equivalent mathematical statements of the boundary conditions are as follows.

$$-k_m \frac{\partial T}{\partial z_{z=0}} = 0 \tag{2.24}$$

$$\frac{\partial T}{\partial r_{r=0}} = 0 \tag{2.25}$$

$$T(r{=}\infty, z, t) \;=\; 0 \tag{2.26}$$

$$T(r, z{=}\infty, t) \;=\; 0 \tag{2.27}$$

$$T(r, z, t{=}0) \;=\; 0 \tag{2.28}$$

2.2.4 Solution procedure for steady state temperature

The solution of equation (2.23) is initiated by use of the integral Hankel transform of zeroth order. The Hankel transform is as follows [6]:

$$\Theta(\lambda,z) = \int_0^\infty T(r,z)\, r\, J_o(\lambda r)\, dr \tag{2.29}$$

where Θ is the eigenfunction. And the inversion formula is:

$$T(r,z) = \int_0^\infty \Theta(\lambda,z)\, \lambda\, J_o(\lambda r)\, d\lambda \tag{2.30}$$

By using the zeroth order Hankel transform, the boundary conditions of equations (2.25) and (2.26) are automatically satisfied. The Hankel transform can be applied to both sides of equation (2.23) to give the following ordinary differential equation.

$$\frac{d^2\Theta}{dz^2} - \Theta(\lambda^2 + \frac{\omega \rho_b c_b}{k_m}) + \frac{BI_o}{4k_m}e^{-\lambda^2\sigma^2/8}e^{-zB} = 0 \tag{2.31}$$

Thus the partial differential equation in r and z is reduced to an ordinary differential equation in z. The total solution to equation (2.31) is the sum of the homogeneous and particular solutions. Solving for Θ and using the inversion formula gives the solution for the temperature distribution as:

$$T(r,z) = \int_0^\infty \lambda J_o(\lambda r)\, \{\, C_1 e^{-z\beta} + C_2 e^{z\beta} - \frac{BI_o\sigma^2 e^{-\lambda^2\sigma^2/8}}{4k_m(B^2-\beta^2)}e^{-zB}\,\}\, d\lambda \tag{2.32}$$

To complete the solution the constants of integration C_1 and C_2 must be determined from

the boundary conditions. Equation (2.27) dictates that C_2 is zero. Equation (2.32) along with the boundary condition of equation (2.24) is used to solve for C_1 to give the complete solution for the steady state temperature distribution.

$$T(r,z) = \frac{I_o \sigma^2 B}{4 k_m} \int_0^\infty \lambda J_o(\lambda r) \, e^{-\lambda^2 \sigma^2/8} \left\{ \frac{B}{\beta} e^{-z\beta} - e^{-zB} \right\} \frac{d\lambda}{B^2 - \beta^2} \qquad (2.33)$$

Equation (2.33) was first presented as a solution for the temperature in laser irradiated tissue with blood perfusion by [28].

The dimensionless form of equation (2.33) is:

$$\theta = \frac{B_\times}{4} \int_0^\infty \lambda J_o(\lambda r_\times) \, e^{-\lambda^2/8} \left\{ \frac{B_\times}{\nu} e^{-z_\times \nu} - e^{-z_\times B_\times} \right\} \frac{d\lambda}{B_\times^2 - \nu^2} \qquad (2.34)$$

$$B_\times = \sigma B$$

The dimensionless variable, $B_\times$, is a ratio of the laser beam radius to the characteristic optical penetration depth.

If there is convection at the tissue surface, the integration constant, C_1, can be resolved. It is assumed that the temperature of the air above the tissue surface is equal to the baseline tissue temperature. The boundary condition of equation (2.24) becomes:

$$k_m \frac{\partial T}{\partial z}\bigg|_{z=0} = h \, T(r, z=0) \qquad (2.35)$$

where h is the heat transfer coefficient. The effects of natural convection as well as forced convection can be accounted for with h. The steady state solution with convection at the surface is:

$$T(r,z) = \frac{I_o \sigma^2 B}{4 k_m} \int_0^\infty \lambda J_o(\lambda r) \, e^{-\lambda^2 \sigma^2/8} \left\{ \frac{B k_m + h}{\beta k_m + h} e^{-z\beta} - e^{-zB} \right\} \frac{d\lambda}{B^2 - \beta^2} \qquad (2.36)$$

Equation (2.36) was first presented as a solution for the temperature in perfused, laser irradiated tissue with surface convection by [29].

The dimensionless form of equation (2.36) is:

$$\theta = \frac{B_x}{4} \int_0^\infty \lambda J_o(\lambda r_x)\, e^{-\lambda^2/8} \left\{ \frac{B_x + Bi}{v + Bi}\, e^{-z_x v} - e^{-z_x B_x} \right\} \frac{d\lambda}{B_x^2 - v^2} \tag{2.37}$$

2.2.5 Solution procedure for transient temperature

The solution for the transient temperature distribution follows a parallel procedure to the steady state case. Again, the solution procedure is initiated by use of the Hankel transform of zeroth order. The Hankel transform is applied to both sides of equation (2.23) to give:

$$\frac{\partial^2 \Theta}{\partial z^2} - \Theta \beta^2 + \frac{BI_o}{4k_m} e^{-\lambda^2 \sigma^2/8} e^{-zB} = \frac{1}{\alpha} \frac{\partial \Theta}{\partial t} \tag{2.38}$$

A Laplace transform of equation (2.38) gives an ordinary differential equation:

$$\frac{d^2 \theta}{dz^2} - \theta \beta^2 + \frac{1}{p} \frac{BI_o}{4k_m} e^{-\lambda^2 \sigma^2/8} e^{-zB} = \frac{1}{\alpha} p\, \theta \tag{2.39}$$

where θ is the eigenfunction and p is the eigenvalue of the Laplace transform. The complete solution of equation (2.39) is the sum of the homogeneous and particular solutions.

$$\theta = \frac{\alpha B I_o\, e^{-\lambda^2 \sigma^2/8}\, e^{-zB}}{4k_m p\, (p + \beta^2 \alpha - B^2 \alpha)} + C_1 e^{-z\sqrt{p/\alpha + \beta^2}} + C_2 e^{z\sqrt{p/\alpha + \beta^2}} \tag{2.40}$$

The constants of integration are evaluated from the boundary conditions. From the boundary condition of equation (2.27), C_2 must be zero. The constant C_1 is found from boundary condition of equation (2.24). The solution for the transient temperature is the inverse Hankel transform of the inverse Laplace transform. The inverse Laplace transform is given below. The details of the inversion are found in Appendix A. The temperature distribution is thus.

$$T(r,z,t) = \frac{BI_o\sigma^2}{8k_m}\int_0^\infty \lambda J_o(\lambda r)\frac{e^{-\lambda^2\sigma^2/8}}{(B^2-\beta^2)}[\frac{B}{\beta}\{e^{-\beta z}erfc(\frac{z}{2\sqrt{\alpha t}}-\beta\sqrt{\alpha t})$$

$$-e^{\beta z}erfc(\frac{z}{2\sqrt{2\alpha t}}+\beta\sqrt{\alpha t})\}$$

$$-e^{-\alpha t(\beta^2-B^2)}\{e^{-zB}erfc(\frac{z}{2\sqrt{\alpha t}}-B\sqrt{\alpha t})-e^{zB}erfc(\frac{z}{2\sqrt{\alpha t}}+B\sqrt{\alpha t})\}$$

$$+2e^{-zB}\{e^{-\alpha t(\beta^2-B^2)}-1\}]\,d\lambda$$

(2.41)

Equation (2.41) must of course be evaluated numerically. Note that as time goes to infinity, equation (2.41) becomes equation (2.33).

Chapter 3

Evaluation of the Bioheat Transfer Model

The results of the previous chapter can be used to help design and optimize the laser perfusion measurement system. The model can be used to determine the experimental parameters (such as surface versus volumetric absorption, optical penetration, laser beam radius, etc.) which maximize the surface temperature sensitivity to changes in perfusion. However, first, to gain confidence in the solution of the model, a comparison is made to the finite element method.

3.1 Comparison with the Finite Element Method

The comparison is made with a commercially available finite element software package called *NEKTON* (from *Nektonics, Inc*, Cambridge. MA). The software uses the spectral element method with a first order Euler backward scheme [35]. The software was run on a CRAY-2/4-256 supercomputer with UNICOS as the operating system.

A finite element mesh consisting of one three dimension element with 100 nodal points and no perfusion was used for all computer simulations. The non-dimensional formulation was used with the element size truncated at r_x and z_x equal to 10.

Figures 3-1 and 3-2 show θ versus r_x and z_x for NEKTON and the exact solution for the case of surface absorption of the laser energy. While the agreement between the solutions is not complete, the solutions are within the error for the finite element method (of the order of the square of the nodal spacing).

Figures 3-3 and 3-4 show θ versus r_x and z_x for NEKTON and the exact solution for the case of volumetric absorption of laser energy. Again, the agreement between the
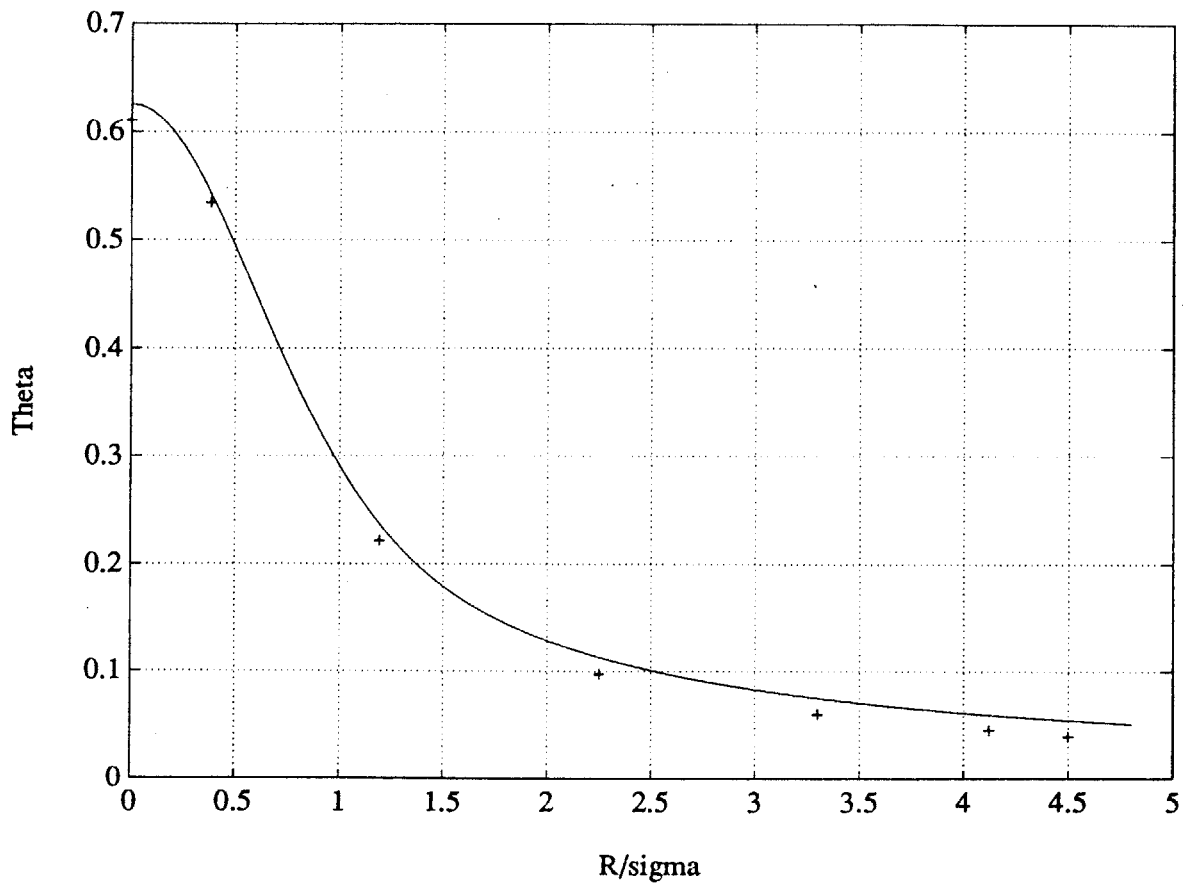
Figure 3-1: A comparison with NEKTON of the temperature at z/σ
equal to zero for surface absorption of laser energy.
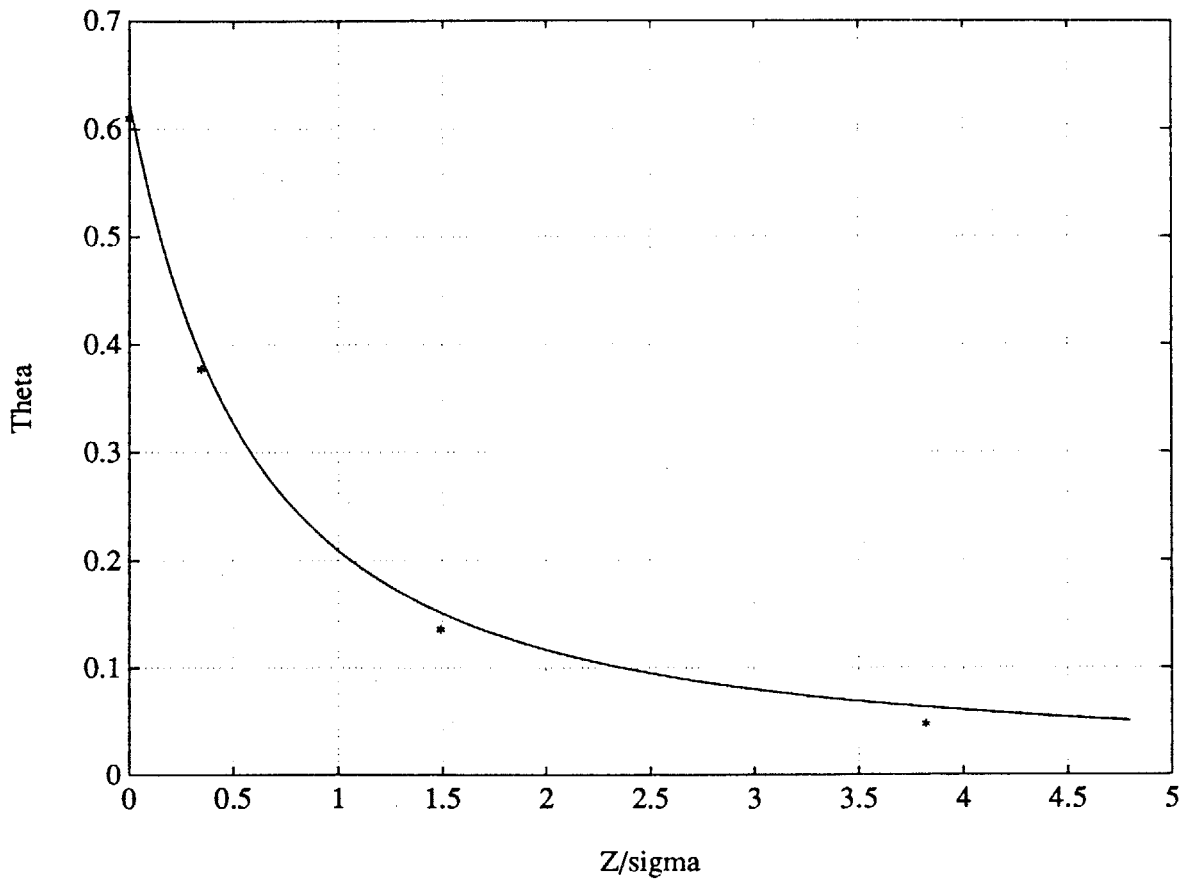
Figure 3-2: A comparison with NEKTON of the temperature at r/σ
equal to zero for surface absorption of laser energy.

solutions is not complete, but the solutions are within the error for the finite element method.

3.2 Predicted Effect of Perfusion on Laser Heating

In this section, the model and solution are used to evaluate the dependence of the temperature field on perfusion.

3.2.1 Surface Absorption of Laser Energy

Figure (3-5) shows the steady state temperature as a function of normalized depth for the case of surface absorption. There are two main observations to be made. One is that for surface absorption of the laser energy, the temperature rise is greatly attenuated in the z direction. Second is that increasing the perfusion to very high flow rates has little effect on the temperature field.

3.2.2 Volumetric Absorption of Laser Energy

For volumetric absorption, the decreasing of the attenuation coefficient, B, causes perfusion to take on greater significance. The temperature as a function of depth into the tissue for a penetrating laser is shown in Figure (3-6) and (3-7). Note that the temperature rise is less attenuated and thus perfusion has a greater effect on the temperature field. The penetration depth of the laser energy in Figure (3-7) corresponds to a Nd-YAG laser incident on soft tissue.

3.2.3 Surface Temperature Dependence on Perfusion

Figures 3-7, 3-6 and 3-5 demonstrate that the temperature field due to volumetric heating is more dependent on perfusion than the temperature field due to surface heating. In the laser based measurement of perfusion, this greater dependence of the temperature field and thus the surface temperature can be exploited to maximize the measurement
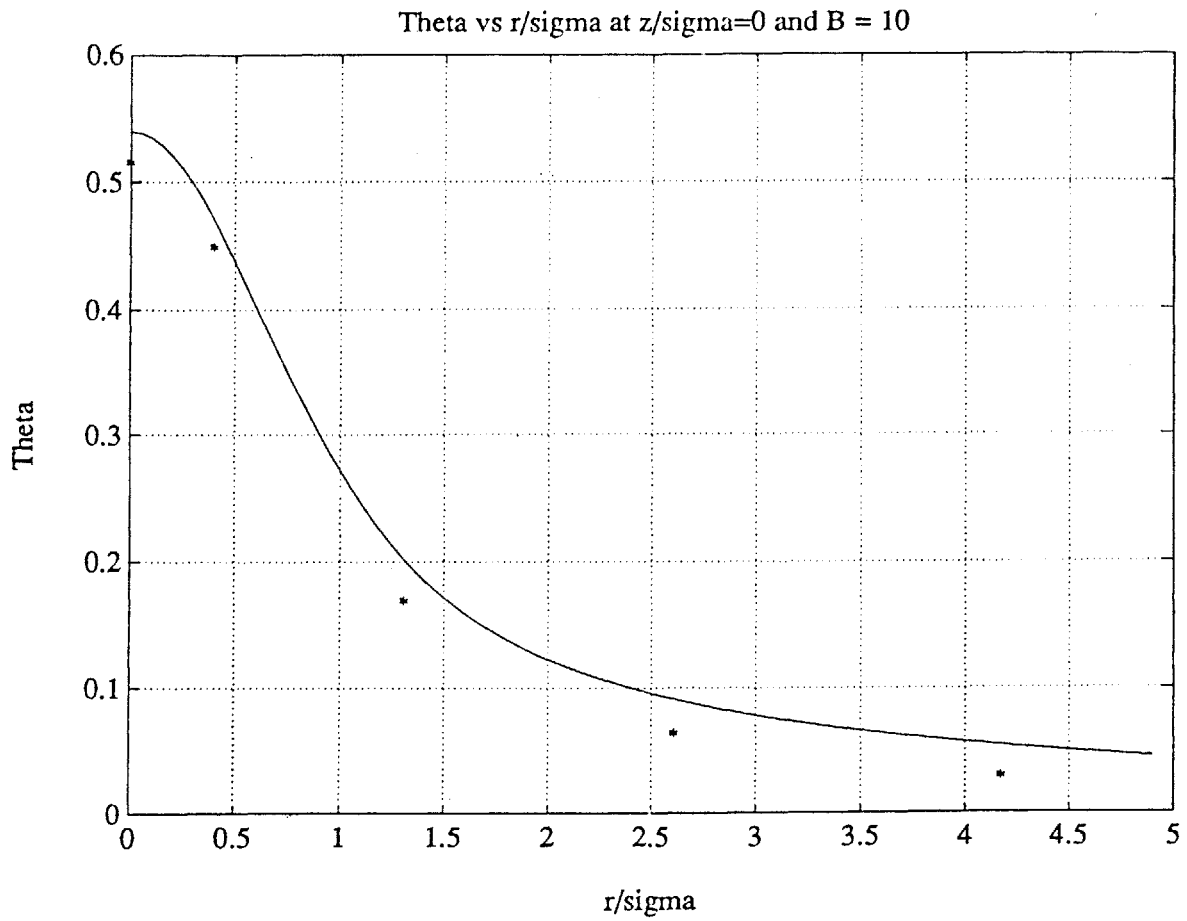
Figure 3-3: A comparison with NEKTON of the temperature at z/σ
equal to zero and Bσ equal to 10 for volumetric absorption
of laser energy.

Theta vs z/sigma for B = 10
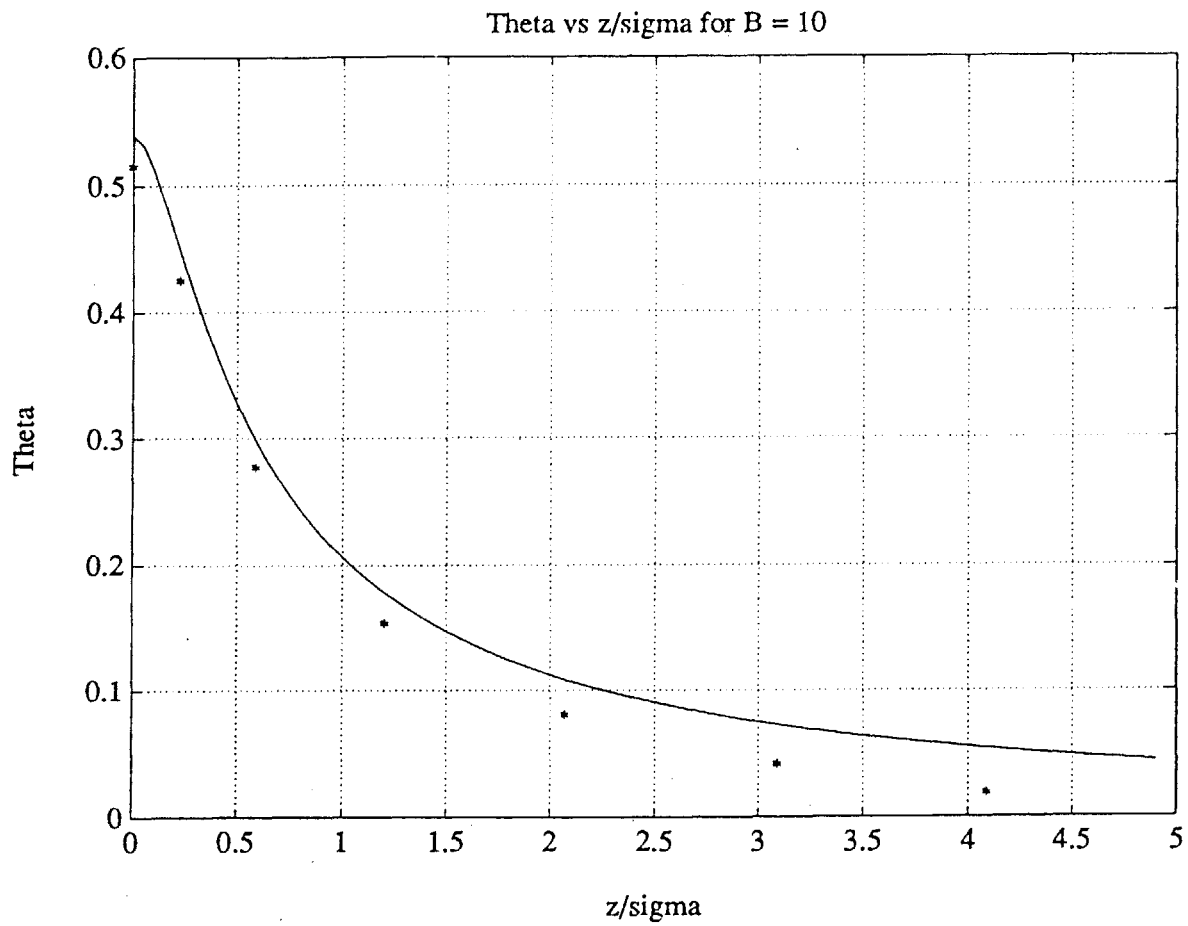
Figure 3-4: A comparison with NEKTON of the temperature at r/σ
equal to zero and Bσ equal to 10 for volumetric absorption
of laser energy.

Surface absorption of laser energy
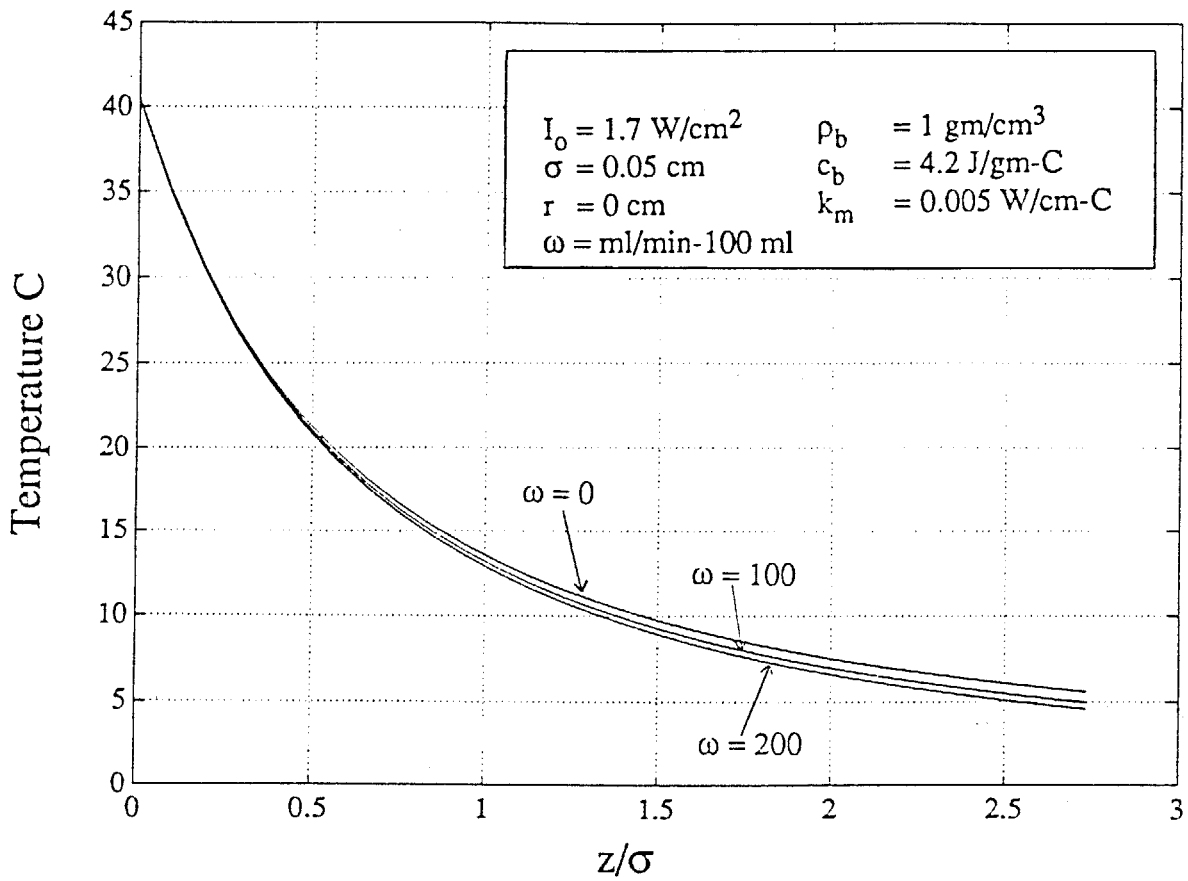
Figure 3-5: The temperature as a function of depth for the
case of surface absorption with blood perfusion.

Volumetric absorption of laser energy

The plot shows Temperature C (vertical axis, 0 to 30) versus z/σ (horizontal axis, 0 to 3).

Parameter box:

$I_o = 1.7$ W/cm^2
$\sigma = 0.05$ cm
$B = 50$ cm^{-1}
$r = 0$ cm

$\rho_b = 1$ gm/cm^3
$c_b = 4.2$ J/gm-C
$k_m = 0.005$ W/cm-C
$\omega = $ ml/min-100 ml

Curves labeled $\omega = 0$, $\omega = 100$, $\omega = 200$.
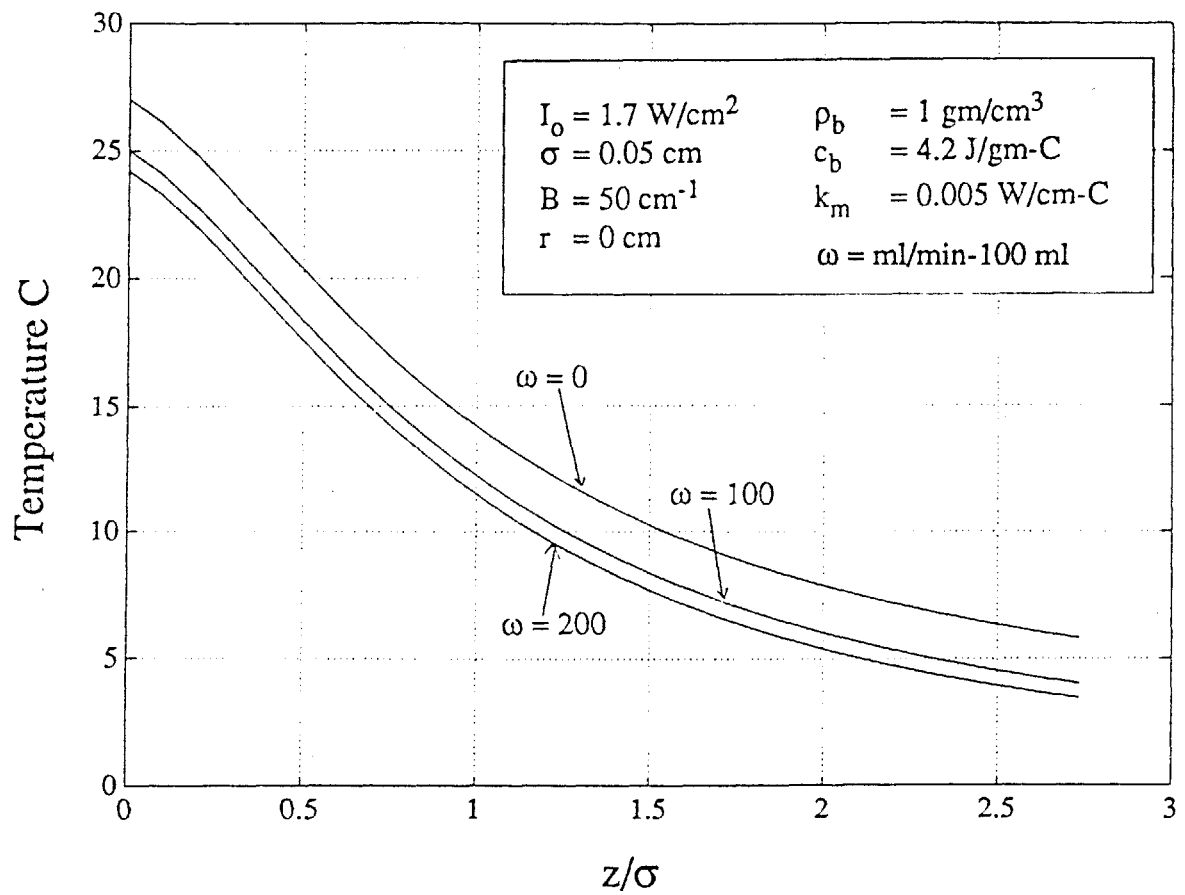
Figure 3-6: The temperature as a function of depth for $B=50$ cm^{-1} with blood perfusion.

Volumetric absorption of laser energy
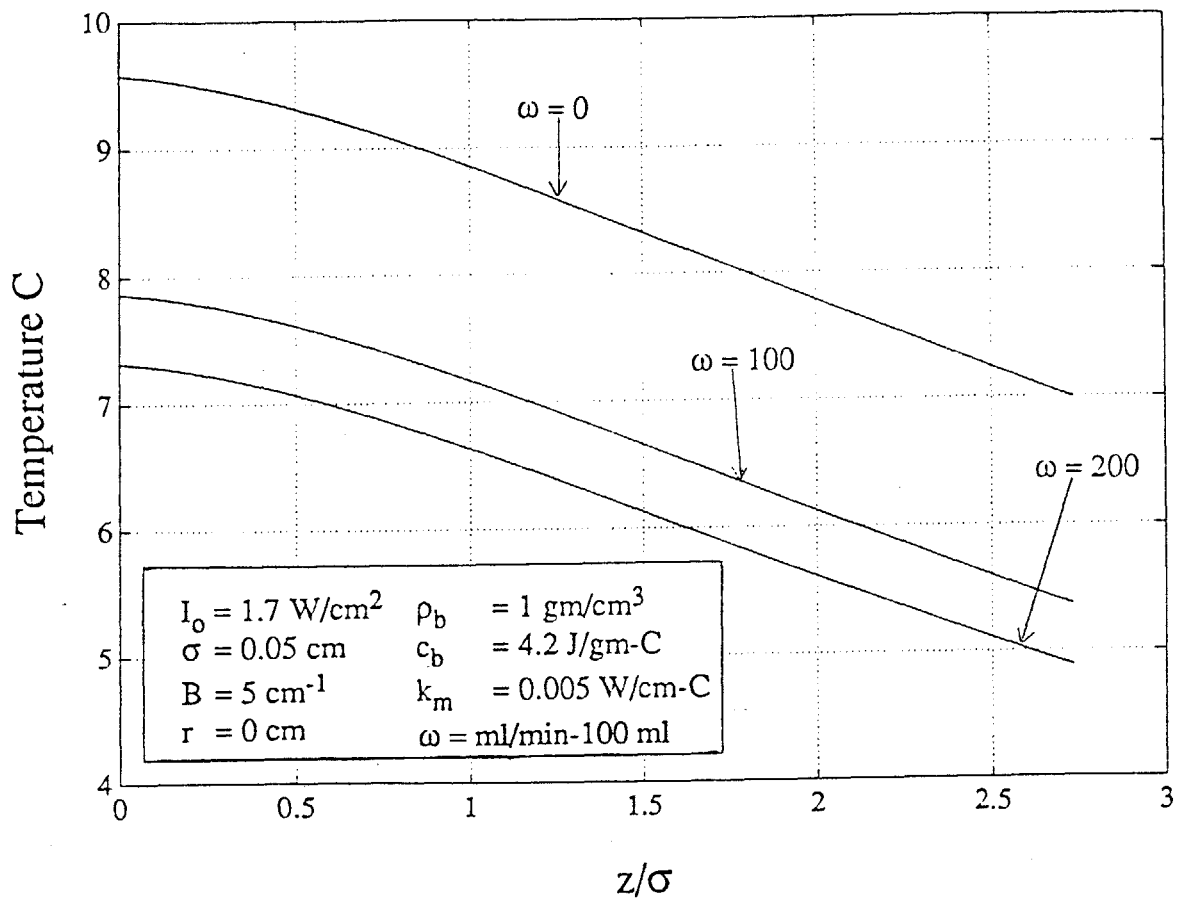
Figure 3-7: The temperature as a function of depth for
$B=5$ cm^{-1} with blood perfusion.

sensitivity to perfusion. The model can also be used to determine the limits of perfusion resolution given a certain temperature measurement resolution. Since there are two possible modes of temperature sensing, the infrared detector and the thermistor, the limit of perfusion resolution will be discussed in terms of the temperature resolution of these sensors.

Figure 3-8 shows the sensitivity of the temperature at r equal to zero at the tissue surface. The family of curves is for different optical penetrations into the tissue which give the same steady state temperature rise (11.3 C). It is evident that the greatest sensitivity of perfusion to surface temperature is obtained when the optical penetration is greatest (or the optical attenuation is least). There are two limits on increasing the sensitivity. One limit is the size of the tissue volume which perfusion is to be measured over. As the penetration increases, so does the heated volume of tissue. Thus a limit is placed on the optical penetration by the desired size of heated tissue volume (which is also the tissue volume over which perfusion is measured). The second limit on increasing the sensitivity is the actual physical limit of light attenuation in tissue.

Once a proper optical attenuation has been selected (by selecting the corresponding laser frequency) and the mode of surface temperature measurement has been selected, the perfusion resolution can be determined. Note that this determination of resolution must take into account the fact that these temperature transducers will measure an *average* temperature over their sensing area. For the case of thermistor temperature measurement, the thermistor must be placed on the tissue surface *outside* the field of view of the laser. This is necessary to avoid thermal artifact in the thermistor. Figure 3-9 shows the percent resolution of perfusion as a function of perfusion for thermistor temperature sensing. It has been assumed that the thermistor has a temperature resolution of 0.005 °C. The figure shows that at low flow rates, a perfusion measurement with a resolution of about 7 percent is possible and at high perfusion rates the resolution increases to about 2 percent. The

Sensitivity of temperature to perfusion
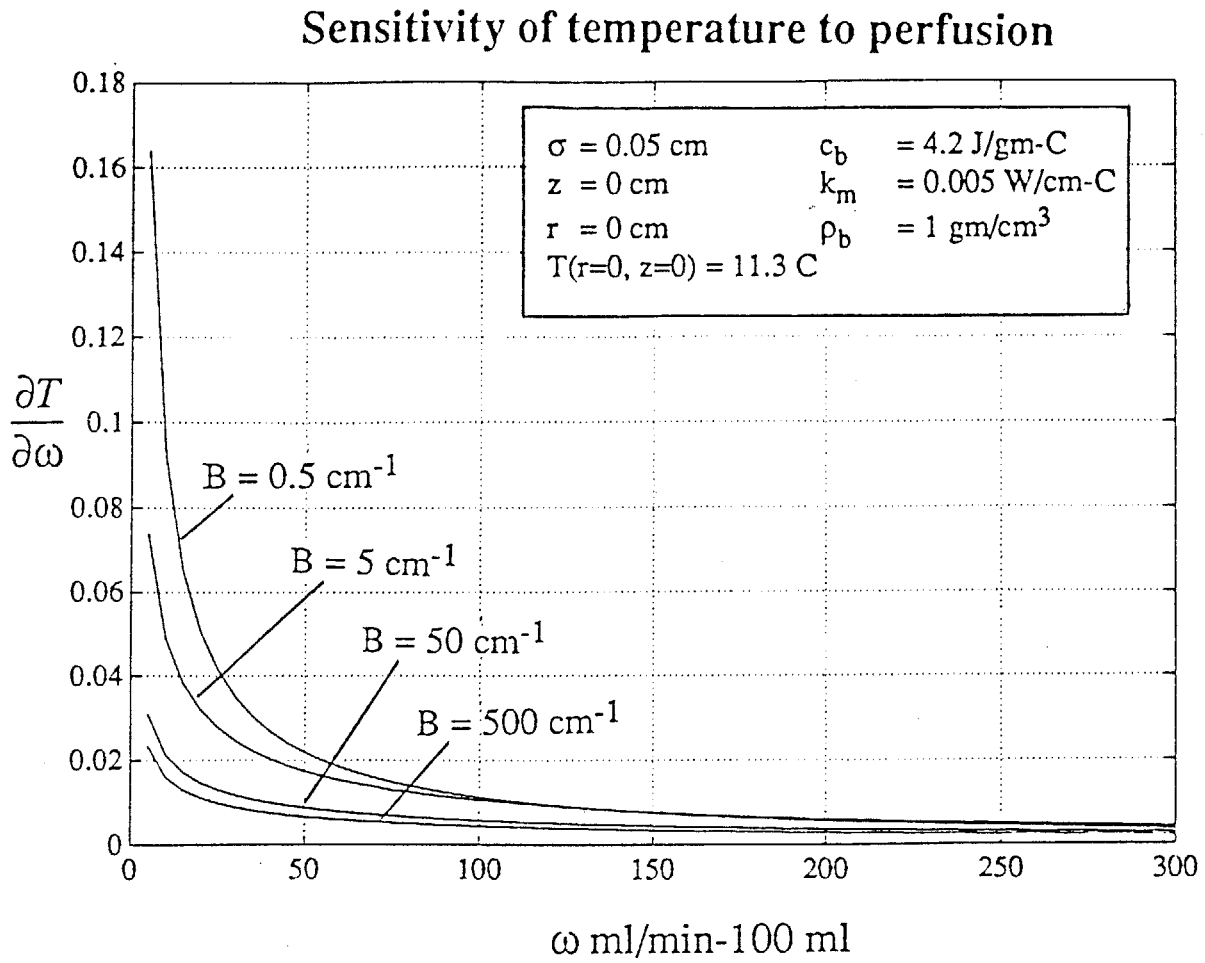
Figure 3-8: Sensitivity of surface temperature to perfusion as a function of
perfusion for a family of optical attenuation coefficients.

model suggest that the laser based measurement of perfusion has a greater perfusion measurement resolution than other measurement systems.

For the case of temperature measurement by infrared detection, the fiber is positioned in close proximity to the tissue surface. The fiber can be focused onto the laser spot if proper optical filtering is done at the detector. Figure 3-10 shows the resolution of perfusion measurement as a function of perfusion for infrared temperature measurement. It has been assumed that the detector system has a temperature resolution of 0.05 $^{\circ}$C. At low flow rates, the resolution is poor (about 40 percent) and at high flow rates the resolution increases to a usable value of about 10 percent.
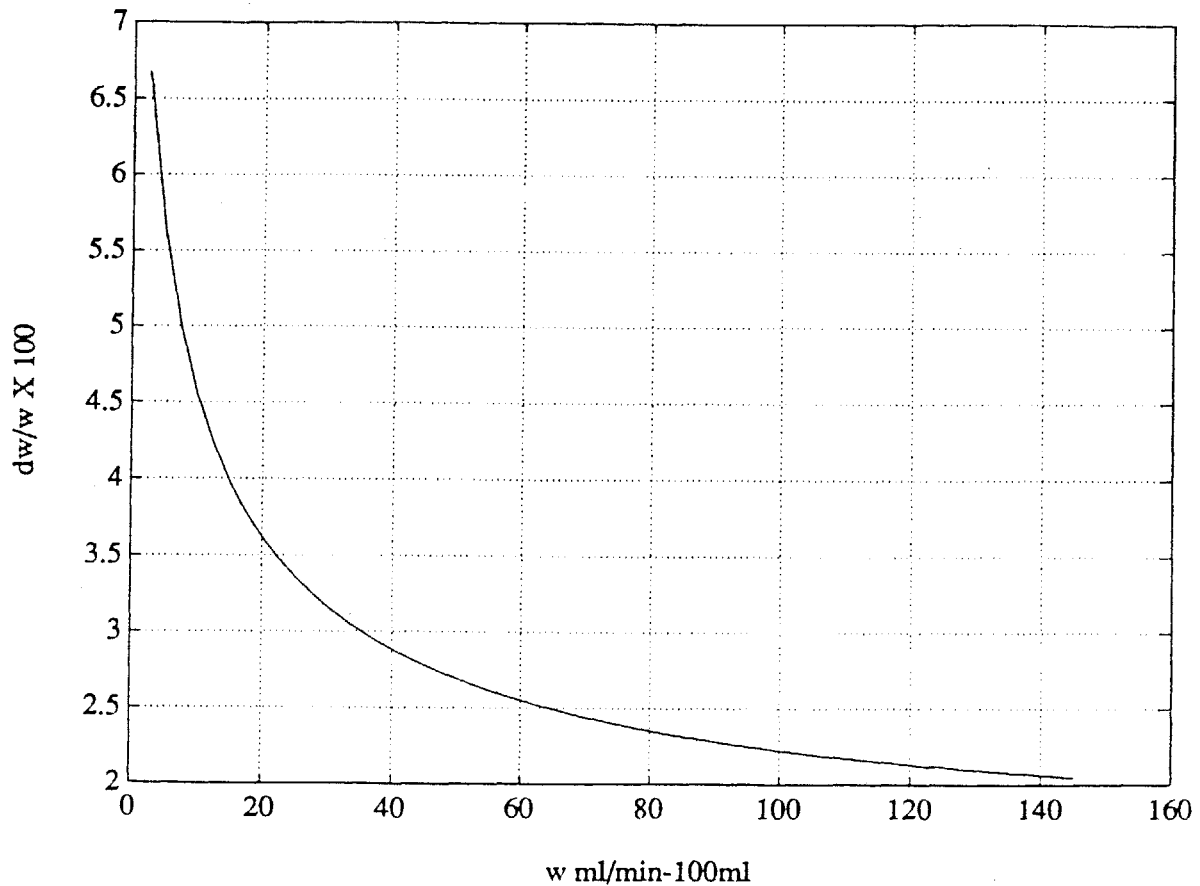
Measurement Resolution for Spherical Thermistor vs Perfusion

$I_o = 2.64$ W/cm^2 ρ_b = 1 gm/cm^3

σ = 0.05 cm c_b = 4.2 J/gm-C

B = 12 cm^{-1} k_m = 0.005 W/cm-C

z = 0 cm   a   = 0.025 cm

dT   = 0.005 C

Figure 3-9: Perfusion measurement resolution for a thermistor mounted on the
tissue surface at r/σ equal to 2.
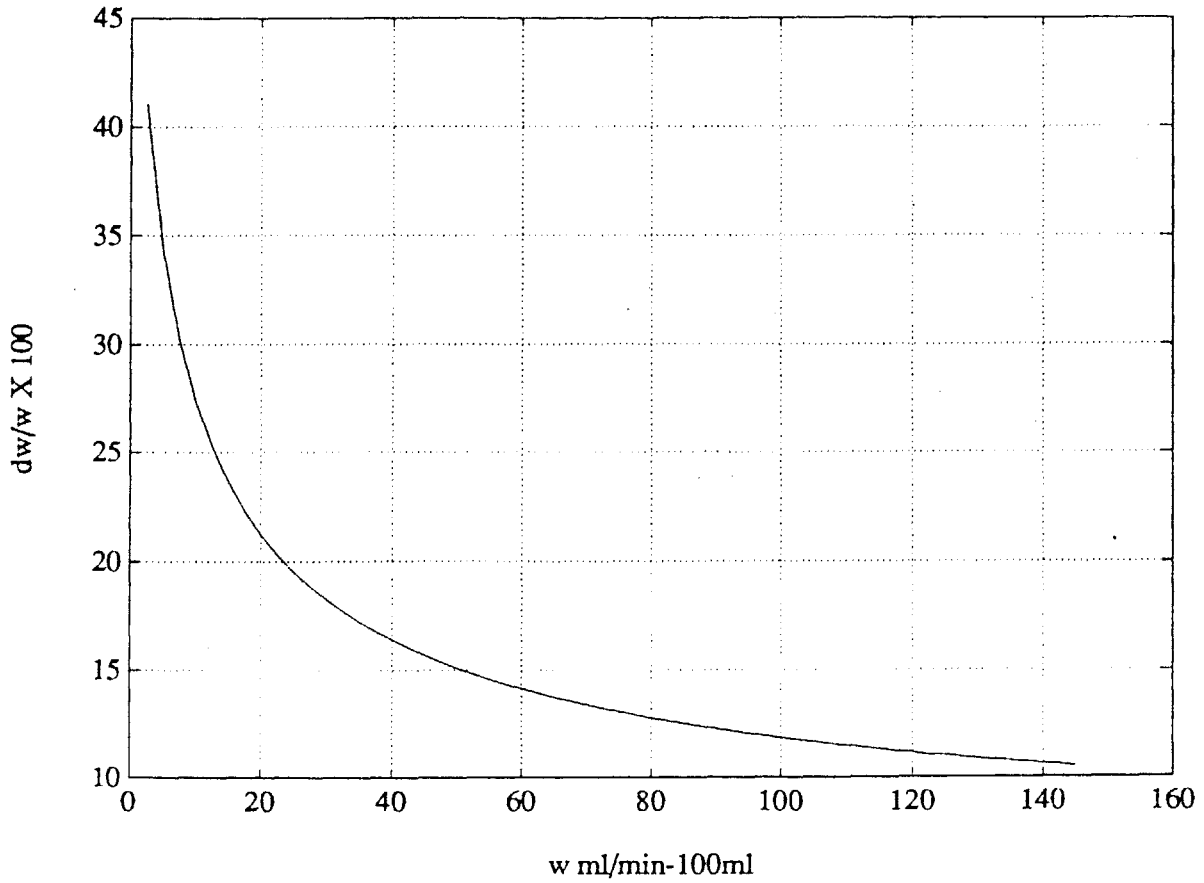
Measurement Resolution for IR Detector vs Perfusion

$I_o = 2.64\ W/cm^2$	ρ_b	$= 1\ gm/cm^3$
$\sigma = 0.05\ cm$	c_b	$= 4.2\ J/gm\text{-}C$
$B = 12\ cm^{-1}$	k_m	$= 0.005\ W/cm\text{-}C$
$a = 0.05\ cm$	dT	$= 0.05\ C$

Figure 3-10: Perfusion measurement resolution for the infrared temperature measurement mode.

Chapter 4

Experimental Protocol, Results and Discussion

In this chapter the experimental protocol and the experimental results for the laser based, non-invasive measurement of perfusion are presented. For the experiment, the temperature rise in a laser irradiated rat liver is recorded for a range of perfusion rates. The surface temperature of the liver is measured on-contact with a thermistor. The purpose of the experiment is to test the validity of the thermal model presented in Chapter 2 and to determine the sensitivity of surface temperature to perfusion.

4.1 Experimental Protocol

The entire experimental protocol includes the procedure for the liver fixation in an ethyl alcohol (ROH) solution, the measurement of the laser beam power, and the measurement of the temperature rise of the laser irradiated liver. A rat liver, fixed in ROH, is perfused by a constant flow pump, with a solution of methylene blue and distilled water. The perfusion everywhere in the liver is assumed to be equal to the average perfusion in the liver. Further, the optical properties of the liver are assumed to be dominated by the optical absorption of the methylene blue solution. Thus the optical absorption and the perfusion are known. The liver is heated by a dye laser tuned to a selected wavelength. The temperature rise of the liver surface is measured for a variety of perfusion rates and the measurements are compared to the thermal model of Chapter 2.

4.1.1 Rat Liver Fixation

The purpose of using an ROH fixed rat liver as a tissue phantom for this perfusion measurement study is as follows.
- The fixed liver provides a medium which when perfused, exhibits heat transfer

properties similar to living tissue in terms of intrinsic thermal conductivity and convective cooling by perfusion.

- The flow of perfusate to the fixed liver can be controlled and quantified.

- The fixed liver can be stored for long periods of time and used repeatedly.

The steps for liver fixation are as follows. This method is taken from [17].

1. An albino rat (*Rattus norvegicus albinus*) is anesthetized with an injection of 0.3 ml of pentobarbital sodium.

2. An incision is made in the from the lower abdomen to the thorax.

3. The portal vein is cannulized with the perfusate supply line (Krebs-Ringer bicarbonate solution with 4% mannitol).

4. The superior vena cava is cannulized with an outflow catheter.

5. The inferior vena cava is sutured closed.

6. The connective tissue surrounding the liver is cleared and the liver is removed.

7. The liver is perfused with Ringer's solution for 20 minutes (*Harvard Apparatus, Inc.* constant flow pump Model 77).

8. The liver is then perfused with 50% ethyl alcohol (ROH) until the vascular resistance decreases.

9. The perfusion pressure is monitored with a pressure transducer (*Omega Engineering, Inc.* Series PX236) and the flow rate is adjusted such that the pressure remains below 120 mm of Hg.

10. The liver is immersed in a 50% ROH solution for 4-6 hours.

11. The liver is perfused with 80% ROH for 15-45 minutes.

12. The liver is then stored in a solution of 80% ROH (indefinite time period).

13. Later to prepare the liver for an experiment, the liver is placed in a 50% ROH solution for 8-10 hours.

14. To rehydrate the liver, it is next placed in distilled water for 8-10 hours.

During the experiment, the liver is perfused with a solution of distilled water and methylene blue (concentration of 0.05 gr/l). This perfusate is used because the peak absorption of the methylene blue occurs within the wavelength range of the heating laser. Thus the extinction of the light is dominated by absorption of photons and not scattering of photons. The absorption dominated light extinction is consistent with the Beer's Law model of radiation attenuation on which the thermal model of Chapter 2 is based. The

absorption spectrum of the methylene blue solution was measured with a *Hewlett-Packard Spectrophotometer 9153A*. At the operating point of the laser, 626 nm, the absorption has a local maximum of 7.37 ± 0.14 cm^{-1}.

4.1.2 Laser Heating

A rhodamine filled dye laser (*Coherent, Inc.*), pumped with an argon laser (*Coherent, Inc.*) is used for the laser heating. The dye laser is tuned to the 626 nm wavelength. This dye laser is used because of its good power stability and beam quality. The laser light is delivered to the liver by a single multimode optical fiber 600 μm in radius. A beam expander is placed at the distal end of the fiber to give the laser beam a radius of 0.6 cm at the tissue surface. The laser power is monitored with a thermal disk laser power meter (*Coherent, Inc.*, Model 210). The laser power incident on the tissue is maintained at about 200 mW.

4.1.3 Temperature Measurement

A thermistor is a temperature dependent resistor. Thermistors are used in this application because of their high accuracy and good resolution. The temperature measurements are made with a thermistor probe (300 μm diameter) and its associated data acquisition hardware (*Thermal Technologies, Inc.; Cambridge, MA; Model TDP 100*). Data are stored and processed on an IBM compatible PC laptop computer.

The thermistor is calibrated with a *Hewlett-Packard Quartz Thermometer Model 2804 A* and the data set is fit with a third order *log* function [47]. The relative temperature resolution is limited by the data acquisition hardware to 0.0035° C.

Temperature measurements are made on the liver surface because this is where the temperature rise depends most on perfusion. Further, in order to avoid specific absorption of the laser energy by the thermistor, the thermistor is mounted on the tissue surface,

outside the field of view of the laser. The liver is suspended from a micro-positioner with a positioning resolution of 0.5 mm and positioned relative to the laser beam. The steady state temperature rise of the liver surface is measured for a range of flow rates, while keeping the laser power and the thermistor position constant.

4.2 Experimental Results and Discussion

Figure 4-1 shows the temperature rise from laser heating (200 mW) at a point on the tissue surface (R = 1.1 cm) for a range of perfusion rates. The solid line represents the thermal model and the symbols represent the experimental data. The perfusion rate during the experiment is assumed to be equal to the average perfusion over the entire liver. Thus perfusion is given by the flow rate of the constant flow pump divided by the volume of the liver (22.9 ml).

From Figure 4-1 it is evident that the agreement between the model and the data is closer at higher rates of perfusion, or lower temperature rises, than at lower rates of perfusion, or higher temperature rises. There are many contributing factors to the mismatch between the model and the data. Some of these factors will be presented and discussed below.

For the experiment, it was assumed that the perfusion is homogeneous over the entire liver and that the perfusion rate is equal to the average perfusion in the liver. Studies have shown [51] that the perfusion in an unheated, ex-vivo rat liver can vary by as much as 100%. During the experiment, however, the homogeneous perfusion was qualitatively verified by the relatively uniform coloring of the liver by the methylene blue solution. Also, since the model agreement is better at higher values of perfusion, at which one would expect greater spatial perfusion variations, the use of the average liver perfusion seems acceptable. Future experiments should incorporate a means of independently measuring the absolute tissue perfusion for a complete comparison with the thermal model.
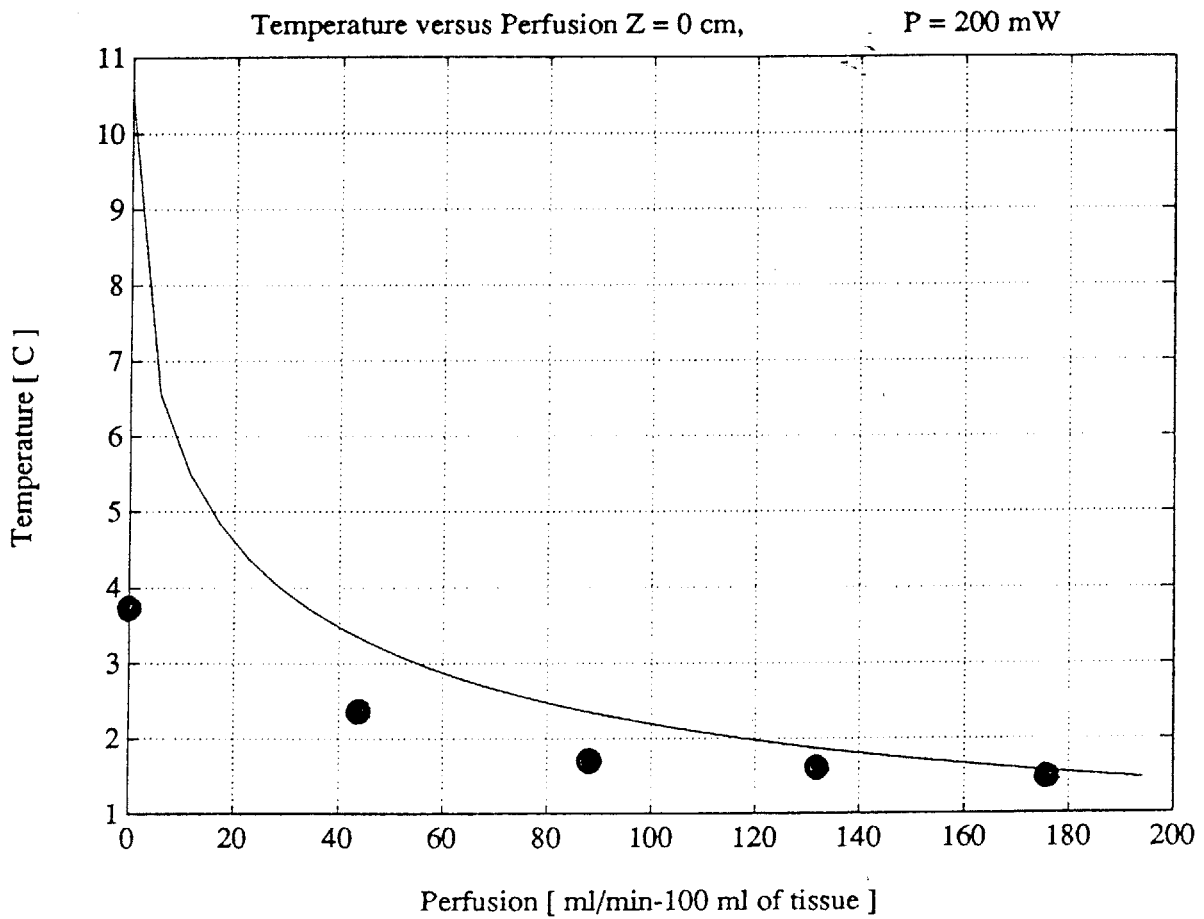
Figure 4-1: The temperature rise on the surface of the liver at R = 1.1 cm and 200 mW of laser power. The solid line represents the thermal model and the symbols represent data.

During the experiment, the laser power was periodically monitored throughout the experiment. It was found that the laser power was stable to less than 10%. The dimensional analysis of the laser heating as presented in Chapter 2 shows that the laser power is directly proportional to the temperature rise. Thus the 10% fluctuations in laser power are not significant enough to account for the mis-match.

For the model, the tissue optical properties have been assumed to be equal to the optical properties of the perfusate as measured on the spectrophotometer. This assumption is valid if the absorption of the perfusate is much greater than the absorption and the scatter of the fixed liver tissue. The measurement of liver optical properties has been carried out by some investigators [37, 33], however these studies refer to $ex\text{-}vivo$ rat liver and human liver respectively. Thus the extrapolation of these data to fixed rat liver is questionable. While the laser wavelength and the perfusate dye have been chosen such that the perfusate absorption dominates any scatter, experimental verification of this claim should be obtained. Another source of error is that the thermal properties of the liver used in the model have been taken from the literature. Yet it has not been established that the thermal properties of the fixed and subsequently re-hydrated tissue equal that of $ex\text{-}vivo$ tissue. However, since the major component of the $ex\text{-}vivo$ and re-hydrated tissue is water, it is expected that the thermal properties are approximately equal. Future experiments should make an independent measurement of the thermal properties of the fixed tissue.

The thermistor temperature measurement system has an excellent measurement resolution (0.0035 °C). Therefore the measurement resolution of the thermistor does not account for the model mis-match. The thermal model presented in Chapter 2 assumes that the tissue surface is adiabatic. In order to be consistent with this model, the thermistor must also be adiabatic. This assumption is supported by the fact that the thermal conductivity of the thermistor material (about 0.1 W/m-K) is significantly lower than the conductivity of the tissue (about 0.5 W/m-K). Another issue which must be confronted is the thermistor

contact resistance with the tissue. Heat flowing through the thermistor will cause a temperature drop at the thermistor-tissue interface if there is a finite contact resistance. The temperature drop prevents the thermistor from measuring the true tissue temperature. In our case, the contact resistance should not cause a significant temperature drop because of the adiabatic nature of the thermistor.

The thermal model presented in Chapter 2 assumes that the tissue surface is adiabatic. The main cause of the model mis-match is most likely due to a violation of this assumption. Heat is transferred out of the tissue surface primarily by natural convection and evaporation. The air in the environment of the liver is still, thus there is no forced convection. Also, since the temperature rise of the liver above the environment is small, radiation heat transfer is negligible. In Chapter 2, the thermal model has also been formulated for the case of heat convection at the tissue surface. One can estimate an average natural convection heat transfer coefficient and obtain with the model the temperature rise for the liver. Such an analysis revealed that at low perfusion rates the difference with and without convection at the surface is no more than 0.5 °C and at high perfusion rates the difference is negligible. Thus natural convection does not play a significant role in the model mis-match.

During the experiment, it was noticed that the ROH fixation had dissolved the endothelial lining surrounding the liver. Consequently, the liver was slowly "sweating" perfusate out of the lobes. This sweating kept the liver surface wetted during the experiment. Presumably, water evaporated off the liver causing a heat flux out the surface. This heat flux is contradictory to the thermal model of Chapter 2. While it is not possible to accurately model the temperature field during evaporation, it should be noted that the mis-match is about equal to the wet bulb temperature difference [44] (about 5 °C) for air with a 50% relative humidity. Thus the model mis-match can be accounted for in terms of the evaporation. In future experiments, the effects of evaporation should be negated. One way

of achieving this is to heat the liver while it is in an environment of 100% relative humidity. Another method is to coat the liver with a thin layer of transparent sealant - in essence restore the dissolved endothelium.

Chapter 5

Summary and Conclusion

The focus of this thesis is to develop a complete methodology for the laser based, non-invasive measurement of blood perfusion. It was shown in Chapter 1 that perfusion is an essential component for the heat and mass transfer in tissue. Thus perfusion is important in the delivery of nutrients to the tissue and the thermoregulation of the tissue. The quantification of perfusion can be used as a systematic measure of the tissue's ability to transport heat and nutrients. It was shown that knowledge of the tissue's ability thermoregulate itself is essential for the successful hyperthermia treatment of neoplastic tumors. Also, it was shown that quantitative knowledge of the tissue transport is necessary for the viability assessment of transplanted tissue. The quantification of perfusion can also be used to diagnose a variety of cardiovascular disorders of compromised flow. Historically, perfusion measurement as a method of diagnosis has not been utilized due to the lack of reliable and accurate measurement methods.

The non-invasive measurement is desirable over invasive techniques because it does not mechanically perturb the tissue and the risk of infection is reduced. The previous work on the laser based measurement of thermal properties and perfusion was discussed. The present work seeks to develop and emphasize the quantification of perfusion as opposed to the quantification of thermal properties or the qualitative assessment of perfusion.

5.1 Model for Thermal Response of Laser Irradiated Tissue

In order the quantify perfusion using a thermal dilution technique, a heat transfer model of the tissue thermal interactions must be made. In Chapter 2, a model and solution for the thermal response of laser irradiated tissue is presented. The model assumes that heat is dissipated in the tissue according to the Pennes formulation of the bioheat transfer equation. This formulation has found wide use and acceptance due to its simplicity and success in describing local tissue heat transfer.

The model is developed for two cases of laser-tissue interaction. The first case is for the surface absorption of all laser energy. The assumption of surface absorption is valid for a middle infrared laser incident on a tissue with a high water content, or a UV laser incident on a tissue with a high protein content. The second case is for the volumetric absorption of laser energy according to the Kubelka-Munk theory of radiation transmission. The assumption of volumetric absorption of laser energy is widely applicable to many different combinations of laser-tissue interaction within the visible spectrum.

For both cases of laser-tissue interaction, a solution has been found for the steady state and transient thermal response of the perfused tissue. These solutions are valuable in and of themselves because they provide a complete description of the thermal response of perfused tissue to laser irradiation. Such a description has been long sought after and has only been previously realized in approximate numerical solutions and in solutions to inadequate models.

In Chapter 3 the model solution is verified with a commercially available finite element software package. The agreement is within the margin of error of the finite element method. Next in Chapter 3, the model is used to optimize the perfusion measurement method. The perfusion measurement resolution is highly dependent on surface temperature resolution. It is shown in Chapter 3 that the surface temperature is made more sensitive to

perfusion by heating the tissue with a laser that penetrates into the tissue. The depth of laser penetration is, however, limited by the maximum tissue volume to measure perfusion over. Also in Chapter 3, the limit on perfusion resolution is estimated given certain tissue optical properties and a finite surface temperature resolution. The perfusion resolution limit achievable with the non-invasive method has the potential to exceed current commercially available perfusion measurement methods.

5.2 Experimental Verification of the Model

In Chapter 4 the experimental protocol, results and discussion are presented for the perfusion measurement experiment. The experiment focuses on measuring the surface temperature rise for a variety of perfusion rates during laser irradiation. A rat liver is fixed in an ethyl alcohol solution. The fixed liver is later rehydrated, perfused by a constant flow pump, irradiated with a laser and the surface temperature is recorded with a thermistor.

The fixed liver is used as a tissue phantom because it exhibits heat transfer properties similar to living tissue, the perfusion can be controlled and independently quantified, and it can be stored for a period of time and reused. Further the optical properties of the liver are controlled and quantified with the use of a dye, methylene blue, in the perfusate. The laser used has been chosen for its good beam quality, stability, and wavelength in order to support the assumptions of the optical and thermal models. A thermistor was used for the temperature measurements because of its high accuracy, excellent resolution, and small size.

The results of the experiment indicate that the dependence of steady state surface temperature on perfusion is high. This experimental result has been predicted by the model sensitivity analysis presented in Chapter 3. Both model and experiment demonstrate that for a laser which is absorbed in the tissue volume, the tissue surface temperature has a strong dependence on perfusion. This result is one of the major tenants of this thesis. The

surface temperature dependence on perfusion can therefore form the basis for a laser based, non-invasive measurement of perfusion.

The results of the experiment also indicate that there is a mismatch between the model and experiment for the temperature rise at low perfusion rates. The mismatch is as high as 100% for the case of no flow and diminishes to about 10% at high flow rates. In Chapter 4 it is shown that the mismatch is primarily due to the evaporation of perfusate off the tissue surface during the experiment. This evaporation causes a heat flux out of the tissue surface. The existence of the heat flux is in contradiction to the assumptions of the thermal model.

5.3 Directions for Future Investigation

The model and analysis presented here suggests that the non-invasive measurement of perfusion has the potential to be developed into a clinically useful instrument. However, various obstacles remain.

5.3.1 Laser Heating

Clearly, a major advance of the non-invasive method, is the use of a laser to obtain controllable, volumetric heating of the tissue. An end result of this is the tissue surface temperature sensitivity to perfusion is increased. However, the ability to characterize the light intensity within the beam as well as within the tissue is limited. The intensity distribution can deviate from a true Gaussian by a significant amount. Also, optical components in the laser delivery system, such as optical fibers, can cause the beam intensity to deviate.

In practice, it is difficult to well characterize the beam profile. There exist sophisticated methods for profile measurement which use an array of photodetectors. The photodetectors are preferable, especially when good characterization is required.

Further, the ability to characterize the light distribution in tissue is limited. The model of surface absorption is quite valid for a mid-infrared laser incident on soft tissue, however, the temperature from surface absorption is not very sensitive to perfusion. In order to maximize the sensitivity, volumetric laser heating has been employed. To quantify perfusion from the volumetric heating, a model for the light distribution in the tissue must be assumed. The ability of this model to describe the internal heat generation in the tissue places fundamental limits on the thermal model and thus the quantification of perfusion.

5.3.2 Thermistor Temperature Measurement

The advantage of the thermistor temperature measurement is that it is accurate, reliable, and can be easily made. Thermistors are common elements to many engineering labs. The main disadvantages are that thermistors need to be individually calibrated, they need an excitation current, and they can distort the temperature field as well as mask the true temperature of the sample. Specific to the application at hand, the thermistors can absorb scattered light energy thus causing a distorted measurement. To optimize the temperature measurement, a thermistor with low thermal conductivity and low optical absorption should be employed. A possible configuration of a thermistor probe, would place a washer shaped thermistor on the distal end of a fiber optic catheter. The fiber optic would carry the laser light to the remote tissue. The washer thermistor would surround the fiber and insure that the thermistor does not absorb direct laser light. The perfusion measurement is then made by placing the distal end of the catheter in contact the the tissue surface, heating the tissue and recording the temperature rise.

5.3.3 Infrared Detector Temperature Measurement

The virtue of the infrared temperature measurement is in the non-contact manner in which it is made. By not coming into contact with the tissue, the infrared thermal sensing does not influence the temperature field in any way. Further, the temperature measurement

can be made at the focus of the laser heating where the temperature is greatest. The disadvantages include the calibration of the detector, the use of the lock-in-amplifier and optical chopper, and the uncertainty of the area over which temperature is being measured. The field of view of the infrared fibers has about a 17 degree divergence, thus one must know accurately the divergence angle and the distance from the distal end of the fiber to the tissue in order to know the area of sensing. With the addition of these parameters into the measurement, the engineering effort required to achieve the infrared measurement exceeds greatly the advantages afforded by it.

5.3.4 Perfused Tissue Phantom

To simulate effect of perfusion on the local tissue heat transfer, a perfused tissue phantom has been used for the perfusion measurement experiments. This tissue phantom is an ethyl alcohol (ROH) fixed liver from an albino rat. It has been assumed that for what concerns the local tissue heat transfer, the fixed liver is an adequate model. Determination of the validity of the fixed liver model is beyond the scope of this thesis. However, a complete study of the non-invasive measurement of perfusion requires that the perfusion measurements be carried out on an isolated organ model and an *in-vivo* organ model. The isolated organ model [51] maintains the organ viability after removal from the animal for up to three hours. It is thought that the isolated model offers a controllable and measurable perfusion model, while mimicking as closely as possible *in-vivo* studies.

Appendix A

Inverse Laplace Transform

The inverse Laplace transform is the sum of the inverse Laplace transforms of the first and second terms of equation ((A.1)).

$$\theta = \frac{\alpha\sigma^2 B I_o e^{-\lambda^2\sigma^2/8}}{4k_m} \left\{ \frac{e^{-zB}}{p(p+\beta^2\alpha-B^2\alpha)} - \frac{\sqrt{\alpha}B e^{-z\sqrt{P/\alpha+\beta^2}}}{p(p+\beta^2\alpha-B^2\alpha)\sqrt{p+\beta^2\alpha}} \right\} \qquad (A.1)$$

The inverse Laplace Transform of the first term in equation ((A.1)) is taken from [8].

$$\Theta_p = \frac{B\sigma^2 I_o e^{-\lambda^2\sigma^2/8} e^{-zB}}{4k_m(B^2-\beta^2)} \left\{ e^{-\alpha t(\beta^2-B^2)} - 1 \right\} \qquad (A.2)$$

To compute the inverse Laplace transform of the second term of equation ((A.1)), a number of substitutions must be made. These substitutions allow the transform to be simplified in such a way that the inversion formula can be found in a standard Laplace transform table.

$$\theta_h = -\frac{\alpha^{3/2}\sigma^2 B I_o e^{-\lambda^2\sigma^2/8} e^{-z\sqrt{P/\alpha+\beta^2}}}{4k_m p(p+\beta^2\alpha-B^2\alpha)\sqrt{p+\beta^2\alpha}} \qquad (A.3)$$

The substitution:

$$s = p + \beta^2\alpha$$

is the complex translation of the Laplace transform [13].

$$F(p+a) \Rightarrow e^{-\beta^2\alpha t} f(t)$$

$$= -\frac{\alpha^{3/2}\sigma^2 B I_o e^{-\lambda^2\sigma^2/8} e^{-\sqrt{s}z/\sqrt{\alpha}}}{4k_m s(s-B^2\alpha)(s-\beta^2\alpha)}$$

The next substitution:

$$r = \sqrt{s}$$

has the following effect on the Laplace transform [13].

$$\frac{1}{\sqrt{s}} F(\sqrt{s}) \implies \frac{1}{\sqrt{\pi t}} \int_0^\infty e^{-u^2/4t} f(u) \, du \tag{A.4}$$

$$= -\frac{\alpha^{3/2} \sigma^2 B I_o e^{-\lambda^2 \sigma^2/8} \, e^{-rz/\sqrt{\alpha}}}{4k_m \, r^2 (r^2 - B^2 \alpha) \, (r^2 - \beta^2 \alpha)}$$

Finally, the real translation:

$$e^{-br} F(r) \implies f(t-b) \; ; f(t-b) = 0 \; \text{for } t < b$$

gives:

$$= -\frac{\alpha^{3/2} \sigma^2 B I_o e^{-\lambda^2 \sigma^2/8}}{4k_m (r^2 - B^2 \alpha) \, (r^2 - \beta^2 \alpha)}$$

The inverse of the resulting transform is found in [8].

$$\Theta_h = -\frac{\sigma^2 B I_o e^{-\lambda^2 \sigma^2/8}}{4k_m \alpha \beta (B^2 - \beta^2)} \{ B \sinh(\beta \sqrt{\alpha} t) - \beta \sinh(B \sqrt{\alpha} t) \}$$

The real translation is applied:

$$= -\frac{\sigma^2 B I_o e^{-\lambda^2 \sigma^2/8}}{4k_m \alpha \beta (B^2 - \beta^2)} \{ B \sinh(\beta \sqrt{\alpha}(t - z/\sqrt{\alpha})) - \beta \sinh(B \sqrt{\alpha}(t - z/\sqrt{\alpha})) \}$$

Equation ((A.4)) is applied:

$$= \frac{1}{\sqrt{\pi t}} \int_{z/\sqrt{\alpha}}^\infty e^{-u^2/4t} \frac{\sigma^2 B I_o e^{-\lambda^2 \sigma^2/8}}{4k_m \alpha \beta (B^2 - \beta^2)} \{ B \sinh(\beta \sqrt{\alpha}(u - z/\sqrt{\alpha})) - \beta \sinh(B \sqrt{\alpha}(u - z/\sqrt{\alpha})) \} \, du$$

The complex translation is then applied:

$$= \frac{\sigma^2 B I_o e^{-\lambda^2 \sigma^2/8}}{8 k_m (B^2 - \beta^2)} \{ \frac{B}{\beta} e^{-\beta z} erfc(\frac{z}{2\sqrt{\alpha t}} - \beta\sqrt{\alpha t}) - \frac{B}{\beta} e^{\beta z} erfc(\frac{z}{2\sqrt{\alpha t}} + \beta\sqrt{\alpha t})$$

$$- 2 e^{\alpha t (B^2 - \beta^2)} e^{-Bz} erfc(\frac{z}{2\sqrt{\alpha t}} - B\sqrt{\alpha t}) + e^{\alpha t (B^2 - \beta^2)} e^{Bz} erfc(\frac{z}{2\sqrt{\alpha t}} + B\sqrt{\alpha t})$$

Finally both terms are combined to give the complete inverse Laplace transform.

$$\Theta = \Theta_p + \Theta_h$$

$$\Theta = \frac{\sigma^2 B I_o e^{-\lambda^2 \sigma^2/8}}{8 k_m (B^2 - \beta^2)} \{ \frac{B}{\beta} e^{-\beta z} erfc(\frac{z}{2\sqrt{\alpha t}} - \beta\sqrt{\alpha t}) - \frac{B}{\beta} e^{\beta z} erfc(\frac{z}{2\sqrt{\alpha t}} + \beta\sqrt{\alpha t})$$

$$- e^{\alpha t (B^2 - \beta^2)} e^{-Bz} erfc(\frac{z}{2\sqrt{\alpha t}} - B\sqrt{\alpha t}) + e^{\alpha t (B^2 - \beta^2)} e^{Bz} erfc(\frac{z}{2\sqrt{\alpha t}} + B\sqrt{\alpha t})$$

$$+ 2 e^{-zB} (e^{-\alpha t (\beta^2 - B^2)} - 1) \}$$

Appendix B
Infrared Temperature Measurement

The purpose of this appendix is to provide a more detailed description and analysis of the infrared temperature measurement system (InTeMeS) for the interested reader. The InTeMeS is used in the non-invasive measurement of perfusion when a non-contact measurement is desired.

B.1 Infrared Detector

The infrared detector is the heart of the InTeMeS because is provides the basic transduction of infrared energy into electrical energy. The detector is a Mercury-Cadmium-Telluride (HgCdTe) model HCT-100, purchased from *Infrared Associates, Inc.* of Cranbury, NJ. The detector is liquid nitrogen cooled and mounted inside a cryogenic deware. To enhance the sensitivity of the detector and the coupling to the IR fiber, a Zinc Selenide (ZnSe) lens was factory mounted in the detector deware. The addition of the lens enhances the sensitivity in two ways. First, the lens is able to focus the incoming energy onto the small detector area (0.0001 cm^2). Second, the lens temperature is about 77 K because it is mounted in the deware. Thus the lens acts as a "cold filter". A cold filter limits the bandwidth of the incoming radiation and does not contribute significantly to the level of background radiation.

With the cold filter, the detector is sensitive to radiation between 2 and 15 μm of wavelength with a peak sensitivity at 10.8 μm. This spectral response of the HCT-100 is matched to the spectral emission of objects at physiologic temperature. (According to Planck's Law, a temperature of 310 degrees has a peak spectral emission at 10 μm.)

B.2 Calibration

The calibration of the detector response as a function of temperature is accomplished by the use of a black body source with an adjustable and controllable temperature. A black body source is an ideal emitter of radiation (it emits radiation according to the Stefan-Boltzman Law).

There exists some literature on the topic of blackbody sources ([23], [15], [40], [10], and [14]). Most of these articles describe a blackbody source that is either out of the physiologic temperature range or does not have the required precision. Most designs are based on a conical radiation cavity with an open end exposed to the atmosphere and a closed end heated to a controlled temperature.

B.2.1 Precision

The precision requirement of the blackbody source is based on our desire to measure surface temperature to within 0.01 C. This temperature resolution requirement can be used to determine a total emissivity precision for the blackbody source that is necessary for calibration. From Planck's Radiation Law:

$$B = \epsilon \, \sigma \, T^4 \qquad\qquad (B.1)$$
$$dB = 4\epsilon \, \sigma \, T^3 \, dT \qquad\qquad (B.2)$$

where B is the power flux density, ϵ is the wavelength average emissivity of the specimen, σ is the Stefan-Boltzman constant and T is the absolute temperature of the specimen. Given that the temperature resolution is 0.01 C, the power flux density resolution at 300 K is 6.12×10^{-6} W/cm^2. Therefore to calibrate the detector to within 0.01 C, the blackbody source must have a power flux density resolution of less than 6.12×10^{-6} W/cm^2.

The total derivative of flux density as a function of emissivity and temperature is:

$$dB \;=\; \frac{\partial B}{\partial \epsilon} \, d\epsilon \;+\; \frac{\partial B}{\partial T} \, dT \qquad\qquad (B.3)$$

$$dB = \sigma T^4 d\varepsilon + 4\varepsilon\sigma T^3 dT \qquad\qquad (B.4)$$

Equation (B.4) is the fluctuation of power flux density in the calibration device as a function of the calibration temperature and the calibration emissivity. From this equation, we want to determine the minimum precision of the emissivity in the device that is needed in order to calibrate the detector to a temperature precision of 0.01 C. In the device, the calibration temperature uncertainty (dT in Equation (B.4)) is known to 0.001 C. For dB equal to 6.12×10^{-6} W/cm^2 at 300 K, σ is equal to 5.667×10^{-12} W/K^4-cm^2, thus dε is equal to 0.00012. Therefore to calibrate the radiometer to measure temperature within 0.01 C, the emissivity of the calibration device must be know to within 0.00012.

B.2.2 Description of Design

The radiation cavity is an 8 inch long cone made of 1/16 inch copper sheet with an absorbing coating painted on the inside. The cone was fabricated by *Charles Jones Studios, Inc.* of Hyde Park, MA. The open end of the cone is covered with an infrared reflector. The reflector has a small aperture which allows the infrared radiation to escape. The cone is heated by 18 guage nichrome wire coiled around the cone.

B.2.3 Analysis of the Design

Next, presented is an analysis of the design, which will determine the effective emissivity and the uncertainty of the effective emissivity.

B.2.3.1 Effective Emissivity of the Radiation Cavity

The geometry of the cavity, the known emissivity of the cavity absorbing coating and the reflectance of the cavity reflector is used to compute a total emissivity for the radiation cavity. It is assumed that the cavity consists of two ideal, gray body surfaces (the absorber surface and the reflector surface) such that:

$$\varepsilon_i = (1 - \rho_i)$$

where ε_i is the emissivity of surface i and ρ_i is the reflectance of surface i. Also, the surfaces are assumed to each be at a uniform temperature, T_i. The inside of the cone is defined as surface 1 and the reflector is defined as surface 2.

The general expression for a graybody enclosure is:

$$B_i = (1 - \varepsilon_i) \sum_{j=1}^{n} B_j F_{i-j} + \varepsilon_i \sigma T_i^4 \qquad (B.5)$$

where B_i is the power flux density from surface i, F_{i-j} is the geometric radiation factor and n is the number of surfaces. For each of the two surfaces, Equation (B.5) is:

$$B_1 = (1 - \varepsilon_1) B_1 F_{1-1} + (1 - \varepsilon_1) B_2 F_{1-2} + \varepsilon_1 \sigma T_1^4 \qquad (B.6)$$

$$B_2 = (1 - \varepsilon_2) B_1 F_{2-1} + \varepsilon_2 \sigma T_2^4 \qquad (B.7)$$

$$\rho_1 = (1 - \varepsilon_1)$$

$$\rho_2 = (1 - \varepsilon_2)$$

Rearranging terms and solving for B_1 gives:

$$B_1 = \frac{\rho_1 F_{1-2} \varepsilon_2 \sigma T_2^4 + \varepsilon_1 T_1^4}{1 - \rho_1 F_{1-1} - \rho_1 \rho_2 F_{1-2} F_{2-1}} \qquad (B.8)$$

If it is assumed that T_1 is equal to T_2 then Equation (B.8) becomes:

$$B_1 = \frac{\rho_1 F_{1-2} \varepsilon_2 + \varepsilon_1}{1 - \rho_1 F_{1-1} - \rho_1 \rho_2 F_{1-2} F_{2-1}} \sigma T^4 \qquad (B.9)$$

And the effective emissivity is:

$$\varepsilon_{eff} = \frac{\rho_1 F_{1-2} \varepsilon_2 + \varepsilon_1}{1 - \rho_1 F_{1-1} - \rho_1 \rho_2 F_{1-2} F_{2-1}} \qquad (B.10)$$

To evaluate Equation (B.10), the height and radius of the cone, as well as the optical properties must be assumed. The design values are in Table B-I.

The geometry of the cone is derived from a set of dimensions which contribute to a

Table B-I: Design parameters for the radiation cavity.

Height of cone   8 in.
Radius of cone base   2 in.
Radius of aperture   0.25 in.
Emissivity of absorber 0.95
Emissivity of reflector 0.05

good effective emissivity and are easy to work with. The emissivity of the absorber (0.95) is the minimum emissivity of a commercially available absorbing coating in the wavelength region between 2 and 15 μm [12]. The emissivity of the reflector is assumed to be the maximum emissivity of polished aluminum in the wavelength region between 2 and 15 μm [59]. The geometrical factor F_{2-1} is the fraction of surface 2's "view" is taken up by surface 1. Since surface 2 is the base of the cone and all surface 2 "sees" is surface 1, then F_{2-1} is equal to 1. For the other geometrical factors, which are extremely complicated to evaluate, their values are taken from the literature [5].

$F_{1-1} = 0.8$
$F_{1-2} = 0.197$

Substuting these values in Equation (B.10) gives:

$\varepsilon_{eff} = 0.99984$

B.2.4 Uncertainty of Effective Emissivity

The explicit expression for the effective emissivity (Equation (B.10)) can be used to compute the uncertainty of the effective emissivity from the uncertainty of each of the components. Consider ρ_1 and ρ_2 to be the only components for which there may be a significant error, then the first order Taylor expansion of the effective emissivity is.

$$d\varepsilon_{eff} = \frac{\partial \varepsilon_{eff}}{\partial \rho_1} d\rho_1 + \frac{\partial \varepsilon_{eff}}{\partial \rho_2} d\rho_2 \qquad (B.11)$$

Equation (B.10) can be solved for the partial derivatives and substitute in the values of Table B-I to give:

$$d\varepsilon_{eff} = -3.3196 \times 10^{-3}\, d\rho_1 - 1.6 \times 10^{-6}\, d\rho_2 \tag{B.12}$$

In the most liberal estimate, the variation in the absorber emittance (or reflectance) is 0.01. Also, a liberal estimate of the variation in reflector emittance (or reflectance) is 0.1. Substituting these values into Equation (B.12) gives:

$$d\varepsilon_{eff} = 0.000034 \tag{B.13}$$

Thus the effective emissivity is:

$$\varepsilon_{eff} = 0.99984 \pm 0.000034 \tag{B.14}$$

Graybody enclose analysis has shown that the effective emissivity of the radiation cavity is 0.99984. Further, an uncertainty analysis of the effective emissivity has found that for generous variations in the absorber emittance and in the reflector emittance, the effective emissivity varies by less than the minimum allowable amount. Therefore, the blackbody source, as presented here, is capable of being used to calibrate an infrared detector to 0.01 C and will be useful in monitoring the detector signal during temperature measurement.

Biography

Gregory T. Martin was born on December 12, 1966 to Eugene F. and Rosemarie (Gemma) Martin in Providence, Rhode Island. At first, his older brother (Eugene F. the Third), felt the arrival of this new baby to be rather upsetting - having lost his comfortable position as only child. But Eugene, who later in life renounced the formal "Eugene" and adopted instead "Gene", grew accustomed to his smaller companion.

Just about the time that Greg was starting to reep the rewards of being the youngest child (1970), another sibling found his way into the family. Timothy, he was called, was the kind of child who was good at playing the part of the youngest. He was cute, loved attention and he always cried to his mother when he didn't get his way. Having now been placed in the precarious position, of being the middle child, Greg learned independence, self-sufficiency and free thought - all qualities common to middle children.

Like so many future engineers, Greg spent much his of childhood taking things apart; toys, radios, appliances and, of course, clocks. Greg's parents permitted this sort of behavior in the hopes that one day an invention or discovery of Greg's would mean early retirement for them. For the most part, Greg shunned organized and competitive sports and instead engaged in activities like chess playing and newspaper delivering.

In 1980 Greg enrolled in Bishop Hendricken High School in Warwick, Rhode Island. Here, Greg studied French, Biology, Religion, Math, etc. Despite the Catholic education, he was able to maintain and develop his free thought. Finding the formal education at times hollow, Greg took responsibility for his own education and began intensive study of philosophy and literature. He was determined to read all the classics and more. Torn between philosophy and engineering (though these two topics are not as different as they may seem), Greg decided that philosophy could be studied and lived at the same time, where formal education in engineering was required for proficiency. While still in the eleventh grade, Greg decided a life of biomedical engineering was his destiny. In this career path was merged the idealism of philosophy with the pragmatism of engineering.

In 1984 at the age of 17, Greg left Warwick for Boston never to return. He pledged Phi Sigma Kappa and lived in the chapter house for his first year at MIT. After, Greg left the confines of the house and moved in with the love of his life Nancy Palmer. Together they lived as poor students, but happy. Well, most of the time they were happy, like that time... eh, I won't go into it. Anyway, they tried to live the examined life. Not as affected intellectuals, but as genuine, curious humans. Greg received his Bachelor's degree in Mechanical Engineering in June of 1988 from MIT.

Having grown accustomed to poverty, Greg continued in the Mechanical Engineering Department as a graduate student. He was a teaching assistant for the undergraduate thermodynamics course 2.40, during his first term. For his Master's thesis, he worked with Dr. H. Frederick Bowman in the Biomedical Engineering Center. In June of 1991, Greg received his Master's degree. Now with so much experience living below the poverty line, Greg decided to continue even further for the PhD. (Also he didn't want to be less educated than Nancy.)

Meanwhile, Nancy and Greg were doing fine. They had taken a few trips in Europe to Spain, France and Italy, spent a summer in Switzerland. A true appreciation of the humanities is necessary for anyone involved in the life sciences. After a relationship of six years, the two decided to be wed on June 15, 1991 at Mount Holyoke College - and the rest is history.

References

1.   Abramowitz, M. and L.A. Stegun, *The Handbook of Mathematical Functions with Formulas, Graphs and Mathematical Tables*, U.S. Government Printing Office, Washington, D.C., NBS Appl. Series 55, (1964).

2.   Apelblat, A., *Table of Definite and Infinite Integrals*, Elsevier Scientific Publishing, Amsterdam, (1983).

3.   Bowman, H. F., "Estimation of Tissue Blood Flow", In *Heat Transfer in Medicine and Biology*, Plenum, New York, (1984), pp. 193-230, ch. 9.

4.   Bowman, H. F., "Heat Transfer and Thermal Dosimetry", *Journal of Microwave Power*, 16(2), (1981), 121-133.

5.   Buschman Jr., A. J. and C.M. Pittman, "Configuration Factors for Exchange of Radiant Energy between Axisymmetrical Sections of Cylinders, Cones, and hemispheres and their Bases", Tech. report D-944, National Aeronautics and Space Administration, October (1961).

6.   Carslaw, H. S. and J. C. Jaeger, *Conduction of Heat in Solids*, Clarendon Press, Oxford, (1959).

7.   Charschan, S.S., *Lasers in Industry*, Laser Institute of America, Toledo, (1972).

8.   Doetsch, G., *Guide to the Applications of Laplace Transforms*, Nostrand Co., (1961).

9.   Drain, L.E., *The Laser Doppler Technique*, John Wiley and Sons, (1980).

10. Duncan, W. D. et al., "Novel Variable Temperature Blackbody for the Far-Infrared", *Infrared Physics*, 26, (1986).

11. Eichler, J. et al, "Temperature Distribution in Tissue During Laser Irradiation", *Radiation and Biophysics*, (1978).

12. Energy Control Products/3M, *Product Information: 3M Brand ECP-2200 Solar Absorber Coating*, St Paul, Minnesota, (1987).

13. Gardner, M. F. and J. L. Barnes, *Transients in Linear Systems*, John Wiley and Sons, (1945).

14. Geist, J. and J.B. Fowler, "A Water Bath Blackbody for the 5 to 60 C Temperature Range", Tech. report 1228, National Bureau of Standards, October (1986).

15. Grigoreva, A. F. et al., "Low-temperature IR Emitter", *Soviet Journal of Optical Technology*, 52, April (1985).

16. Hansen, W. P., R. J. Greenwald, and H. F. Bowman, "Application of the CO_2 Laser to Thermal Properties Measurements in Biomaterials", *ASME Journal of Engineering Materials and Technology*, ASME, November (1973), pp. 295-308.

17. Holmes, K. R., W. Ryan, P. Weinstein, M. M. Chen, "A Fixation Technique for Organs to be used as Perfused Tissue Phantoms in Bioheat Transfer Studies", *Advances in Bioengineering*, R. L. Spilker,ed., ASME, (1984), pp. 9-10.

18. Hudson, R. D., *Infrared System Engineering*, John Wiley and Sons, (1969).

19. Kamada, T., N. Sato, N. Kakubari, K. Yoda, S. Kawano, M. Schichiri, and H. Abe, "Noninvasive Assessment of Microcirculation of Living Organs and Tissues Using Laser", *Lasers in Surgery and Medicine*, 2, (1983), 275-280.

20. Katzir, A., H. F. Bowman, Y. Asfour, A. Zur and C. R. Valeri, "Infrared Fibers for Radiometer Thermometry in Hypothermia and Hyperthermia Treatment", *IEEE Transactions on Biomedical Engineering*, 36, June (1989), 634-637.

21. Keyes, R. J., *Optical and Infrared Detectors*, Springer-Verlag, (1977).

22. Kreith, F. and W.Z. Black, *Basic Heat Transfer*, Harper and Row, (1980).

23. Lee, R. D., "Construction and Operation of a Simple High-Precision Copper-Point Blackbody and Furnace", Tech. report 483, National Bureau of Standards, May (1969).

24. Leung, W. P. and A. C. Tam, "Thermal diffusivity in thin films measured by non-contact single-ended pulsed-laser-induced thermal radiometry", *Optics Letter*, 9, No. 3, March (1984), 93-95.

25. Leung, W. P. and A. C. Tam, "Techniques of flash radiometry", *Journal of Applied Physics*, 56, No. 1, July (1984), 153-161.

26. Long, F. H., N. S. Nishioka, and T. F. Deutsch, "Measurements of the Optical and Thermal Properties of Biliary Calculi Using Pulsed Photothermal Radiometry", *Lasers in Surgery and Medicine*, 7, (1987), 461-466.

27. Luke, Y.L., *Integrals of Bessel Functions*, McGraw-Hill, New York, (1962).

28. Martin, G. T. and H. F. Bowman, "The Temperature Distribution in Laser Irradiated Tissue with Blood Perfusion", *Bioheat Transfer - Applications in Hyperthermia, Emerging Horizons in Instrumentation and Modeling*, American Society of Mechanical Engineers, December (1989), pp. 97-102.

29. Martin, G. T. and H. F. Bowman, "Model and Solution for the Thermal Response of Blood Perfused Tissue during Laser Hyperthermia", *Laser - Tissue Interaction* , S. Jaques,ed., SPIE, The International Society for Optical Engineering, January (1990), pp. 308-316.

30. Martin, G. T. and H. F. Bowman, "The Temperature Distribution in a Semi-infinite Body Due to Surface Absorption of Laser Radiation", *International Communications in Heat and Mass Transfer*, 17(1), January/February (1990), 93-104.

31. Moser, K. M., "Pulmonary Thromboembolism", In *Principles of Internal Medicine*, Plenum, New York, (1977), pp. .

32. Numerical Algorithms Group, *Library Manual Mark 11 Volume 6*, (1984).

33. Nakamura, S., Y. Nishiwaki, S. Suzuki, S. Sakaguchi, Y. Yamahita, K. Ohta, "Light Attenuation of Human Liver and Hepatic Tumors After Surgical Resection", *Lasers in Surgery and Medicine*, 10, (1990), 12-15.

34.   NASA, "Thermal Remote Anemometer Device", Tech. report LAR-13508, Langley Research Center, August (1985).

35.   Nektonics, Inc., *NEKTON Version 2.5 Documentaion*, Cambridge, MA, (1989).

36.   Ozisik, M. N., *Boundary Value Problems of Heat Conduction*, International Textbook, Scranton, Penn, (1968).

37.   Parsa, P., S. L. Jacques, N. S. Nishioka, "Optical Properties of Rat Liver Between 350 and 2200 nm", *Applied Optics*, 28, No. 12, June (1989), 2325-2330.

38.   Partovi, F. et al., "A Model for Thermal Ablation of Biological Tissue Using Laser Radiation", *Lasers in Surgery and Medicine*, 7, (1987).

39.   Patera, A. T., "Application of the Finite Element Method to the Conduction of Heat in Perfusing Tissue", Master's thesis, Massachusetts Institute of Technology, (1980).

40.   Pavlyukov, A. K. et al., "Blackbody for energy calibration of infrared equipment", *Soviet Journal of Optical Technology*, 46, October (1979).

41.   Pennes, H. H., "Analysis of Tissue and Arterial Blood Temperatures in the Resting Human Forearm", *Journal of Applied Physiology*, 1, No. 2, (1948), 93-122.

42.   Ready, J.F., *Effects of High-Power Radiation*, Academic Press, New York, (1971).

43.   Roberts, J. O. and B. M. Jones, "Assessment and Monitoring of Microvascular Free Tissue Transfers", *Clinical Investigation of the Microcirculation*, Meeting on Clinical Investigation of the Microcirculation, London, (1985), pp. 199-224.

44.   W. M. Rohsenow, H. Choi, *Heat, Mass and Momentum Transfer*, Prentice-Hall, Inc., Englewood Cliffs, New Jersey, (1961).

45.   Smits, G. J., R. J. Roman and J. H. Lombard, "Evaluation of Laser-Doppler Flowmetry as a Measure of Tissue Blood Flow", *Journal of Applied Physiology*, 86, August (1986).

46.   Song, C. W., A. Lokshina, J. G. Rhee, M. Patten, and S. H. Levitt, "Implication of Blood Flow in Hyperthermia Treatment of Tumors", *IEEE Transactions on Biomedical Engineering*, BME-31, January (1984), 9-14.

47.   Steinhart, J. S. and S. R. Hart, "Calibration Curves for Thermistors", *Deep-Sea Research*, 15, (1968), 497-503.

48.   Svaasand, L.O., T. Boerslid, and M. Oeveraasen, "Thermal and Optical Properties of Living Tissue: Application to Laser-Induced Hyperthermia", *Lasers in Surgery and Medicine*, 5, (1985), 589-602.

49.   Tajiri, H., "Study of Laser Hyperthermia, Photodynamic Therapy and the Combined Therapy For Human Pancreatic Cancer Cell Line", *Laser Surgery: Characterization and Therapeutics*, The International Society for Optical Engineering, Bellingham, WA, (1988), pp. 37-39.

50.   Takahashi, K., N. Yoshida, and K. Yamauchi, "Silver Halide Infrared Fiber", Tech. report 26, Sumitomo Electric, January (1987).

51.   Valvano, J. W., J. T. Allen, J. T. Walsh et al., "An isolated Rat Liver Model for the Evaluation of Thermal Techniques to Quantify Perfusion", *Journal of Biomechanical Engineering*, 106, August (1984), 187-191.

52.   Valvano, J. W., J. T. Allen and H. F. Bowman, "The Simultaneous Measurement of Thermal Conductivity, Thermal Diffusivity, and Perfusion in Small Volumes of Tissue", *Journal of Biomechanical Engineering*, 106, August (1984), 192-197.

53.   Waldow, S. M., P. R. Morrison, and L. I. Grossweiner, "Nd:YAG Laser-Induced Hyperthermia in a Mouse Tumor Model", *Lasers in Surgery and Medicine*, 8, (1988), 510-514.

54.   Walsh, J. T. , "A Non-Invasive Thermal Method For Quantifying Tissue Perfusion", Master's thesis, Massachusetts Institute of Technology, (1985).

55.   Watson, G.N., *A Treatise on the Theory of Bessel Functions*, Cambridge University Press, London, (1966).

56.   Welch, A. J. and M. Motamedi, "Interaction of Laser Light with Biological Tissue", In *Laser Photobiology and Photomedicine*, Plenum, New York, (1984), pp. 29-53.

57.   Welch, A.J., "The Thermal Response of Laser Irradiated Tissue", *IEEE Journal of Quantum Electronics*, QE-20, (1984).

58.   Welch, A. J., E. H. Wissler, L. A. Priebe, "Significance of Blood Flow in Calculations of Temperature in Laser Irradiated Tissue", *IEEE Transactions on Biomedical Engineering*, BME-27, No. 3, March (1980), 164-166.

59.   Wolfe, W. L., *The Infrared Handbook*, Office of Navel Research, (1978).

60.   Zur, A. and A. Katzir, "Use of Infrared Fibers for Low Temperature Radiometric Measurements", *Applied Physiology*, 40, (1986).